9.2 Dyeing of Aliphatic Polyamides

As discussed, of the three types of synthetic polyamide available (i.e. *aliphatic*, *semi-aromatic* and *aromatic*), linear, aliphatic polyamides and, in particular, PA 6 and PA 66 dominate the global textile market. As PA 6 and PA 66 have received by far the greatest attention from a dyeing perspective (e.g. [7, 9, 178–180]), this discussion focuses on the dyeing of these two types of fibre. Of the manifold dye classes that can be used on PA fibres, the most commercially important are acid dyes, although the use of reactive dyes has increased in recent times. Accordingly, this account focuses primarily on the thermodynamics and kinetics of dyeing PA fibres with both non-metallised acid dyes and pre-metallised acid dyes.

As recounted earlier, the polymer chains in both PA 6 and PA 66 fibres comprise amide groups separated by methylene sequences (—$(CH_2)_n$—) and are terminated by carboxyl (—COOH) groups as well as amino (—NH_2) or acetylamino (—$COCH_3$) groups. From a dyeing perspective, all the major classes of dye are substantive towards the two types of PA substrate. The presence of terminal amino groups imparts dyeability with anionic dyes, namely acid dyes (includ-ing pre-metallised acid dyes), direct dyes, mordant dyes and reactive dyes, the carboxyl end groups accords substan-tivity towards basic dyes, whilst the polar and relatively hydrophobic nature of the polymer imparts substantivity towards disperse dyes; vat dyes, sulphur dyes and azoic colorants can also be applied.

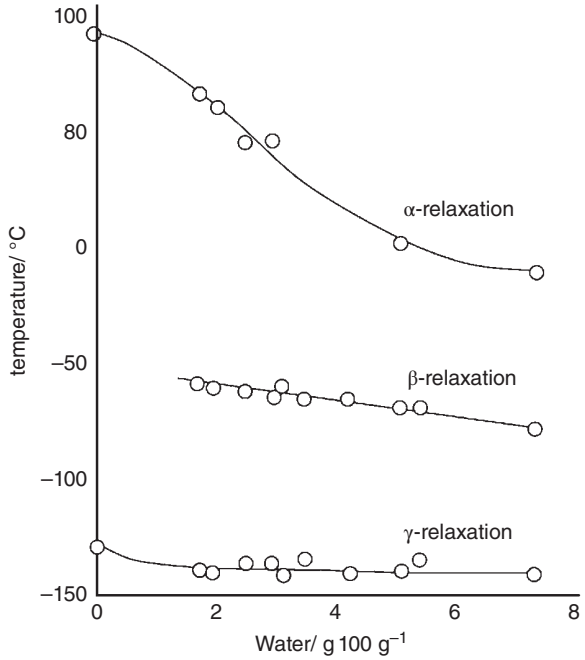

Figure 9.15 Effect of moisture content on the temperature of the relaxations of PA 66. Reproduced from [80], with permission from American Chemical Society.

9.2.1 Effect of Physical Processing on Dyeing

Briefly, in terms of the effects of dry heat setting and steam setting on the dyeing of PA fibres [181–185], whilst both processes increase fibre crystallinity, the latter treatment reduces fibre modulus and increases dye uptake mainly because of decreased orientation whereas dry heat setting reduces AEG content owing to oxidative degradation and decreases dye uptake [9]. Whilst treatment in the presence of water breaks interchain H-bonds, dry heat treatments tend to result in the formation of additional H-bonds [154]. Fibre drawing affects dyeability [186–188] insofar as the rate of dye diffusion is reduced by increasing draw ratio, although equilibrium dye uptake is little affected.

9.2.2 Barré Effects

A significant problem that can occur in dyeing PA fabrics is a striped or barred appearance caused by differences in both the rate and extent of dye uptake within different yarns that comprise a particular fabric. Such inter-yarn non-uniformity, which is commonly referred to as *barré*, can result from both physical and chemical variations. The former type of irregularity is introduced during fibre processing (drawing and heat setting) or stem from variations in crimp or decitex, whilst chemical irregularities arise during fibre spinning or from the blending of yarns of different AEG content [9]. The ability of anionic dyes to cover physical and chemical irregularities in PA fabrics varies (e.g. [189]), which contrasts with the generally excellent coverage of such irregularities displayed by disperse dyes. It is generally considered that chemical variations are nowadays rare [190] and that barré effects arise mostly from physical variations in PA fibres [190, 191]. Holfeld *et al.* propose that such physical variations alter the porosity of the substrate, porosity relating to the regions between crystallites together with the regions between adjacent polymer chains in the amorphous domains [84, 192] and that porosity is determined by the total tension–temperature history of the substrate (i.e. manufacture, texturing, setting, dyeing and finishing) [154, 190]. As such, fibre porosity alters the accessibility of the fibre towards dye molecules [154] and tends to be emphasised by high molar mass, anionic dyes [154].

The previously discussed radial non-uniformity of PA fibres (i.e. skin/core structure) that results from the processing conditions employed during melt spinning has been discussed in the context of barré dyeing. Tracer diffusion studies using labelled dye anions ($D^{35}SO_3^-$) and chloride ions ($^{36}Cl^-$) demonstrated the presence of a surface layer that served as a barrier to acid dye diffusion within PA 66 fibres [87]. Analysis of the diffusional characteristics of the surface and core regions of PA 66 fibres as a function of draw ratio revealed that fibre anisotropy varied with draw ratio insofar as the diffusion coefficient, D_b, decreased with increasing draw ratio, as also did the value of *surface admittance*, α, this being a combination of the dye diffusion coefficient in the surface layer, the layer thickness and the difference in dye substantivity between the layer and the fibre core (Figure 9.16).

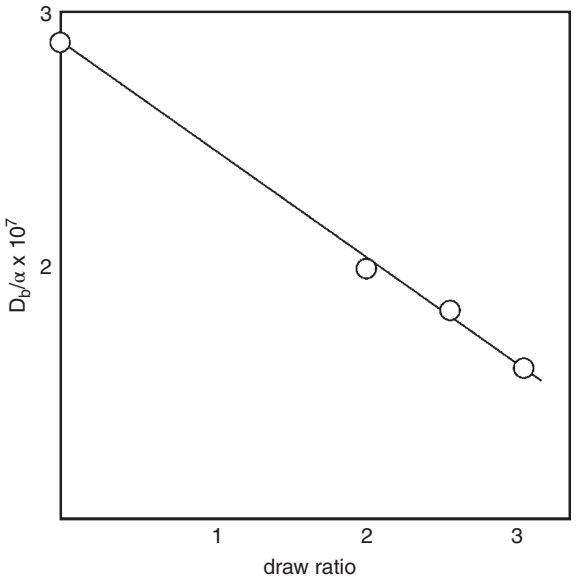

Figure 9.16 Variation of D_b/α as a function of draw ratio. Reproduced from [87], copyright of the Society of Dyers and Colourists.

Generally, barriness arising from physical variations can be minimised or even overcome completely by using yams with the same processing history, employing dyes of high migrating ability, using elevated dyeing temperatures (PA 6: 110–115°C; PA 66: 110–120°C) and/or proprietary levelling agents [9]. Diagnostic tests have been developed that utilise selected types of anionic dye [9, 190].

9.2.3 Levelling Agents

As control of pH and temperature may not be sufficient to achieve level dyeing, recourse is commonly made to proprietary auxiliaries that promote level dyeing (e.g. [193–196]), of which there are three types [9].

9.2.3.1 Anionic Levelling Agents (e.g. [9, 84, 179, 197–200])

These compete with the anionic dyes for sites within the fibre and reduce the rate of dye uptake and promote levelness and coverage of fibre irregularities.

These fibre-substantive compounds are adsorbed on the fibre surface and impart a *blocking* effect to the dye molecules, this being temporary insofar as once adsorbed at the fibre surface, the levelling agents are displaced by the dye anions (Figure 9.17), thereby reducing the initial dye strike. The use of anionic levelling agents or *anionic retarding agents* significantly reduces barré dyeing.

9.2.3.2 Cationic Levelling Agents (e.g. [9, 198, 199, 201–203])

These compounds form a complex with the anionic dye in the dyebath (e.g. [9] and the references therein). The dye anion/cationic agent complex dissociates gradually with increasing temperature during dyeing, which releases dye anions for adsorption on the substrate and thereby reduces the rate of dyeing (Figure 9.18). To prevent precipitation of the dye–cationic agent complex, the addition of a non-ionic levelling agent can be made to the dyebath.

9.2.3.3 Non-ionic Levelling Agents [9, 204–207]

Such compounds form a complex with the anionic dye that reduces the relative amount of dye molecules in the dyebath, thereby retarding dye uptake.

9.3 Acid Dyes

The dyeing of PA fibres with acid dyes was reported soon after the introduction of the fibre (e.g. [191, 208–211]). Whilst the term *acid dye* stems from the use of acidic dyebaths that were originally employed for the application of anionic dyes to wool and silk fibres, some modern acid dyes do not necessarily require the use of acidic dyebaths,

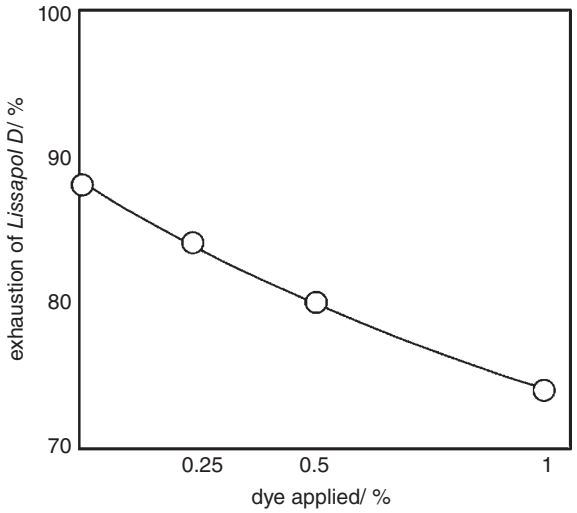

Figure 9.17 Displacement of *Lissapol D* from PA 66 by C.I. Acid Red 266 at 95°C. Reproduced from [200], copyright of the Society of Dyers and Colourists.

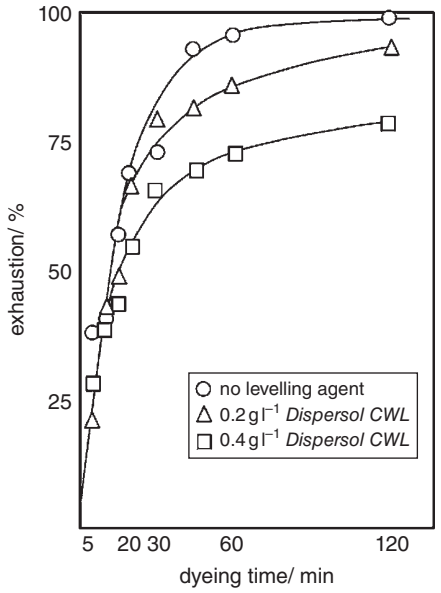

Figure 9.18 Effect of cationic levelling agent (*Dispersol CLW*) on the uptake of C.I. Direct Red 1 at 95°C. Reproduced from [200], copyright of the Society of Dyers and Colourists.

as the dyes display adequate dye–fibre substantivity under neutral pH conditions. Although in the *Colour Index* [212] the *Acid Dye* application class also includes metal complex dyes (aka *pre-metallised acid dyes*), as both dyers and dye chemists consider pre-metallised acid dyes as being distinct from their non-metallised counterparts, the two types of acid dye will be considered separately herein.

In essence, acid dyes are applied to PA fibres from weakly acidic/neutral/slightly alkaline dyebaths, under which conditions, dye substantivity accrues from electrostatic forces of interaction between protonated amino end groups in the fibre $\left(-NH_3^+\right)$ and anionic groups (commonly sulfonate, $-SO_3^-$) in the dye molecules. Other forces of interaction, including H-bonding, dipole–dipole, etc., also contribute.

9.3.1 Non-metallised Acid Dyes

In such dyes, water solubility is conferred by the presence of one or more sulfonate groups ($-SO_3Na$). Non-metallised acid dyes are dominated by azo structures and provide a wide range of hues as exemplified by C.I. Acid Red 266 and C.I. Acid Orange 173, although AQ dyes are also represented such as C.I. Acid Blue 129 : 1.

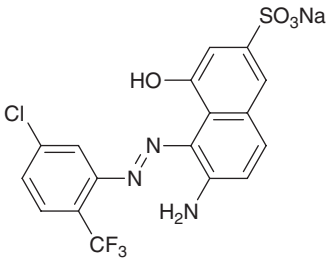

C.I. Acid Red 266

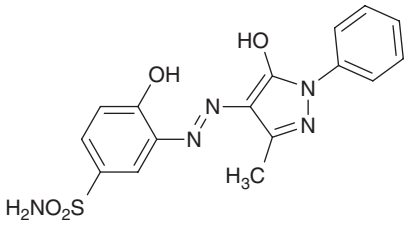

C.I. Acid Orange 173

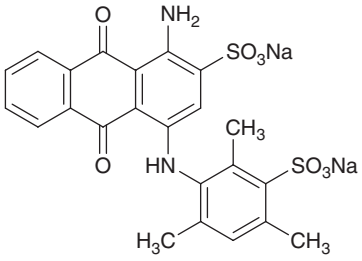

C.I. Acid Blue 129:1

Non-metallised acid dyes vary in terms of their dyeing behaviour on PA fibres [9, 180]. Essentially, large molar mass representatives of low water solubility tend to display high substantivity under neutral pH conditions and exhibit high levels of wet fastness but provide poor coverage of barré. Highly sulfonated variants typically display low substantivity and high migration ability but require acidic application conditions and exhibit low wet fastness properties on PA fibres. The rate of dye uptake onto PA 6 fibres is generally greater than on their PA 66 counterparts because of the greater crystallinity and more compact structure of the latter type of fibre. The pH employed for dyeing varies between ~pH 4 and 8, depending on the type of dye and depth of shade applied [9]. In practice, control of dyebath pH can be achieved using three different approaches, namely the use of relatively high acidity, the utilisation of buffer systems to maintain the pH within a narrow region or the gradual lowering of dyebath pH as dyeing proceeds (e.g. [7, 9, 213, 214]). The dyes are commonly applied at 98°C, although enhanced dye migration can be achieved at elevated temperatures (PA 6: 110–115°C; PA 66: 110–120°C) for coverage of barré. Proprietary levelling agents are commonly used to enhance level dyeing. Owing to the varied dyeing behaviour of non-metallised acid dyes on PA fibres, dye makers often classify members of their dye ranges; Stevens [215] proposed a system of classification based on several dye–fibre characteristics. Despite the continued popularity of this particular dye class on PA fibres, the fastness to wet treatments of dyeings secured using non-metallised variants often leaves much to be desired, and therefore it is customary to after-treat the dyeings using either natural or synthetic tanning agents in order to secure adequate levels of wet fastness [9].

9.3.1.1 Thermodynamics of Dyeing

As mentioned, owing to the presence of amino end groups within the substrate, acid dyes, direct dyes, mordant dyes and reactive dyes are substantive towards PA fibres. In terms of the mechanism by which such dyes are adsorbed onto PA fibres, as the application conditions used for these four types of anionic dye on PA fibres are generally similar insofar as exhaustion is undertaken under acidic or slightly alkaline pH conditions, to a first approximation, the following account of the thermodynamics of the adsorption of non-metallised acid dyes on PA fibres can be assumed to apply to the other three classes of anionic dye.

The adsorption of dye anions onto PA substrates has been interpreted in terms of the adsorption of simple acids and alkalis, obtained in the form of *titration curves*. This approach is analogous to that employed for wool fibres (Chapter 10), which is not surprising in view of the chemical resemblance between PA fibres and protein fibres, notably the presence of both amino and carboxyl groups. Two approaches have been used to analyse the data obtained from titration curves, namely a *specific site* (Langmuir) model first proposed by Gilbert and Rideal in 1944 and various *ion-exchange* models based on modifications of a Donnan membrane theory originally proposed by Peters and Speakman in 1949, again in a manner analogous to that of wool, although the approach adopted for the two types of fibre are slightly different because PA fibres contain an excess of carboxyl groups whereas wool contains an equal amount of amino and carboxyl groups. The principles involved in both the Langmuir and Donnan models are discussed in Chapter 10.

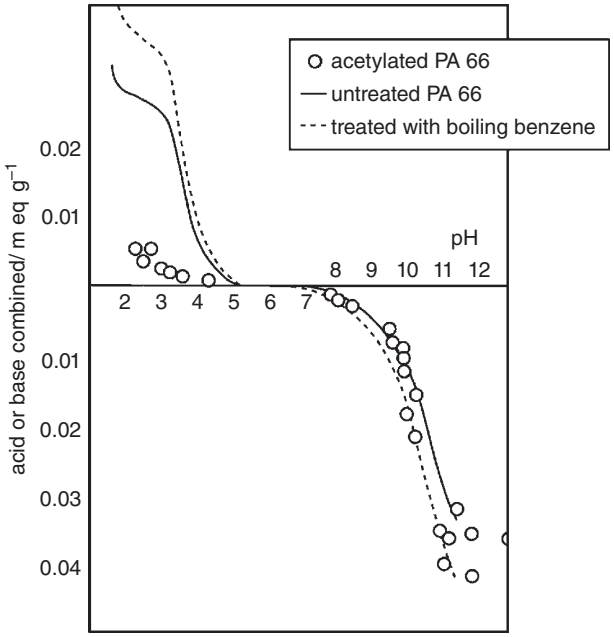

Figure 9.19 Titration curve of PA 66 with HCl and NaOH at 21.5°C (figure 10 on page 2023 of reference [219]). Reproduced from [219], with permission from John Wiley & Sons, Inc.

9.3.1.1.1 Titration Curves The interaction of PA fibres with acids and bases has been a subject of extensive study, the first qualitative investigation having been made by Elod and Schachowsky [216] in 1942. Subsequently, several workers studied the adsorption of various simple acids (e.g. HCl and H_2SO_4 [216–221]) as well as that of more complex acids [219, 220] and NaOH [219, 222]. In the case of HCl and NaOH, the work of Mathieson *et al.* [219] in the case of PA 66 fibre is especially illustrative.

These workers showed that the titration curve of PA 66 with HCl and NaOH (Figure 9.19) comprises two distinct regions, namely one below pH 6 that corresponds to acid adsorption and one above pH 7 that corresponds to the adsorption of alkali, the inflection at pH 6–7 corresponding to the *isoelectric point*[16] of the fibre. Within the acidic region, the titration curve displays an inflection at low pH values (around pH 2–3) that corresponds, approximately, to the AEG content of the fibre. Below pH 2, acid uptake increases, without limit, which has been attributed to adsorption of the acid onto chain amide groups (i.e. ─CONH─) [217–220, 223]. Within the alkaline region, the titration curve exhibits an inflection at ∼pH 12–13, which can be attributed to maximum alkali combination with the carboxyl groups in the fibre.

In terms of the mechanism of acid and alkali adsorption by PA fibres, it is generally considered that at its isoelectric point, PA fibres exist in the zwitterion[17] form (**X**), although because PA fibres typically contain more ─COOH groups than ─NH_2 groups (Table 9.1), the excess carboxyl groups will be undissociated at the isoelectric point and therefore the number of ─COO^- groups present is determined by the number of ─NH_2 groups in the fibre. As acid is added to the isoelectric fibre, (**X**), protons are adsorbed onto the ionised carboxyl groups and the fibre develops a positive charge (**XI**) owing to the protonated amino end groups. Such a process will continue until all the ionised carboxyl groups have been 'back titrated'. The amount of acid adsorbed should therefore be equal to the number of amino end groups in the substrate, and thus acid adsorption should reach a limit. However, as Figure 9.19 clearly shows, at low pH values, acid adsorption does not reach a finite level, but rather continues to increase with decreasing pH [216–219, 224], this having been ascribed to adsorption of protons onto chain amide groups (**XII**) that results in protonation of the amide group (**XIII**).

$$\underset{\textbf{X}}{H_3N^+\text{-nylon-}COO^-} \overset{H^+}{\rightleftharpoons} \underset{\textbf{XI}}{H_3N^+\text{-nylon-COOH}}$$

$$\underset{\textbf{XII}}{\text{-NHCO-}} \overset{H^+}{\rightleftharpoons} \underset{\textbf{XIII}}{\text{-}NH_2{}^+CO\text{-}}$$

[16] the isoelectric point is sometimes abbreviated as *IEP* and the pH at which the parameter occurs is denoted by *pH(I)*, although *pI* is also employed.
[17] see Chapter 5 for a definition.

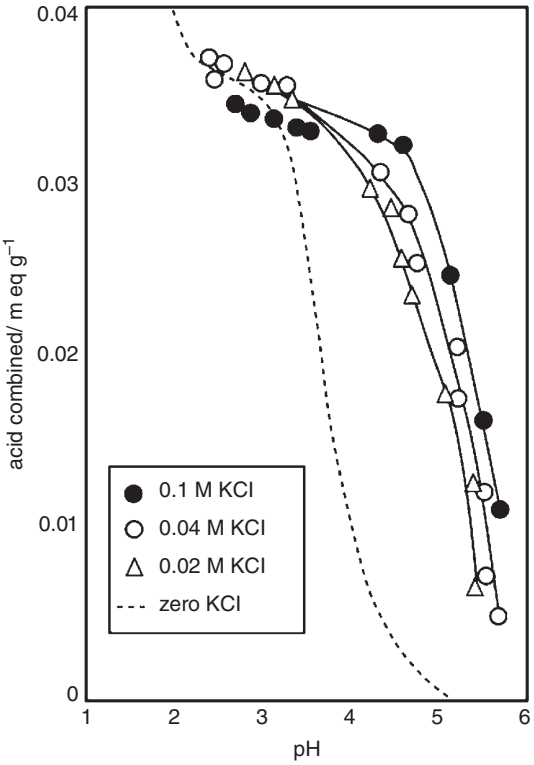

Figure 9.20 Titration curve of PA 66 with HCl at 21.5°C in the presence of KCl. Reproduced from [219], with permission from John Wiley & Sons, Inc.

In the case of the titration of PA fibre with alkali, protons can be removed from the undissociated carboxyl groups (**XIV**) [178, 219, 222]. When all such undissociated carboxyl groups have been ionised, protons are then removed from the protonated AEG in the zwitterion (**XV**) with the result that the fibre carries an overall negative charge (**XVI**). The amount of alkali adsorbed corresponds to the total —COOH group content of the fibre.

$$\underset{\textbf{XIV}}{H_3N^+\text{-nylon-COOH}} \overset{OH^-}{\rightleftharpoons} \underset{\textbf{XV}}{H_3N^+\text{-nylon-COO}^-} + H_2O \overset{OH^-}{\rightleftharpoons} \underset{\textbf{XVI}}{H_2N\text{-nylon-COO}^-} + H_2O$$

The dependence of acid adsorption on the amino end groups was demonstrated by the finding that PA 66 fibres in which most of the —NH_2 end groups had been acetylated displayed much reduced acid uptake (Figure 9.19).

Mathieson *et al.* [219] demonstrated that the addition of electrolyte (KCl) shifted the titration curve to higher pH values (i.e. HCl adsorption at a given pH increased) (Figure 9.20) whilst an increase in temperature slightly reduced the amount of acid adsorbed.

In the case of the titration of PA 66 with more complex acids (Figure 9.21), the curves shift to higher pH values as the size of the anion increases.

The affinity of three such acids (calculated at the pH corresponding to 50% acid adsorption) relative to that of HCl is shown in Table 9.6; as the affinities of the three acids are higher on PA 66, adsorption occurs at higher pH values in the case of the polyamide substrate.

9.3.1.1.2 Analysis of Titration Curves As mentioned, the data obtained from titration curves such as those shown earlier have been interpreted using both a specific site (Langmuir) model (Gilbert–Rideal) as well as various models based on ion exchange (Donnan membrane equilibrium). The principles underlying these two approaches are discussed in Chapter 10. Excellent accounts of the analysis of the titration curves of PA fibres are available (e.g. [178, 217, 225–228]).

As previously recounted, the analysis of the acid titration curves obtained for PA fibres using the Gilbert–Rideal and Donnan approaches is analogous to that employed for wool fibres and reflects the similar chemical nature of PA fibres and protein fibres, notably the presence of both amino and carboxyl groups. However, PA contains far fewer amino groups than wool (Table 9.7), and also PA fibres contain an excess of carboxyl groups whereas wool contains an equal amount of amino and carboxyl groups.

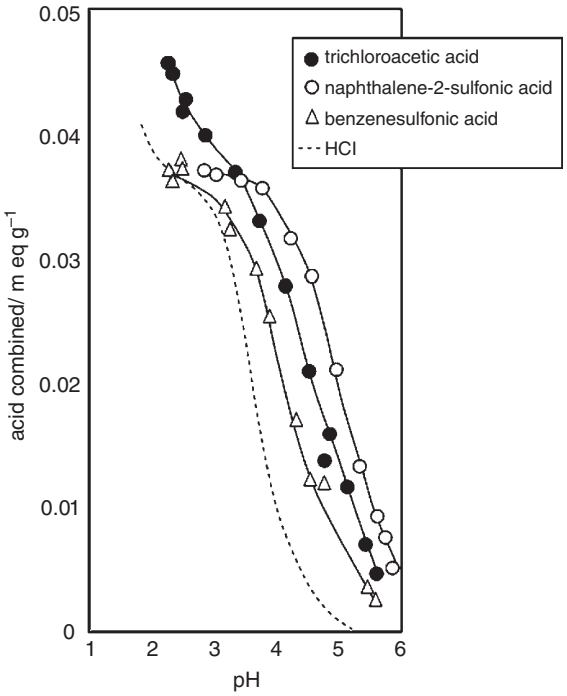

Figure 9.21 Titration curve of PA 66 with various strong acids at 21.5°C. Reproduced from [219], with permission from John Wiley & Sons, Inc.

Table 9.6 Affinity/kJ mol^{-1} at 20°C of various acids relative to HCl [178].

acid	PA 66	wool
Benzenesulfonic acid	9.6	3.4
Trichloroacetic acid	14.2	5.1
Naphthalene-2-sulfonic acid	17.9	10.3

Table 9.7 Amino end groups content of different fibres [229].

fibre	AEG/m eq kg^{-1}
Wool	800–900
Silk	120–200
PA	30–50

The similar behaviour of wool and PA fibres in terms of the dependency of anion affinity on relative anionic mass is shown in Figure 9.22 by the shift in pH required for half-saturation [230].

Gilbert and Rideal (Langmuir) and Peters and Speakman (Donnan) Models Because the adsorption of simple inorganic acids onto PA fibres is analogous, qualitatively, to that of their adsorption on wool, the equations relating to both the Gilbert and Rideal (Langmuir) and Peters and Speakman (Donnan) models discussed in Chapter 10 are applicable, although modifications are required because, as discussed earlier, unlike wool, PA fibres contain more ─COOH groups than ─NH_2 groups. Also, in a manner analogous to wool, discrepancies are observed between experimentally observed findings and theoretical predictions, which, as in the case of wool fibres, can be attributed both to the fibre not being ideally stable, as is assumed in the models and also, perhaps more importantly, to discrepancies that stem from the theoretical treatments themselves.

Excellent detailed accounts of this area are available [178, 217, 228]. Briefly, starting from Eq. 10.7, which was derived for the analysis of the acid titration curves obtained for wool (Chapter 10), in the case of the titration of PA with a monobasic acid, HX, following the approach adopted in Eq. 10.6, values for θ_H and θ_X are given by

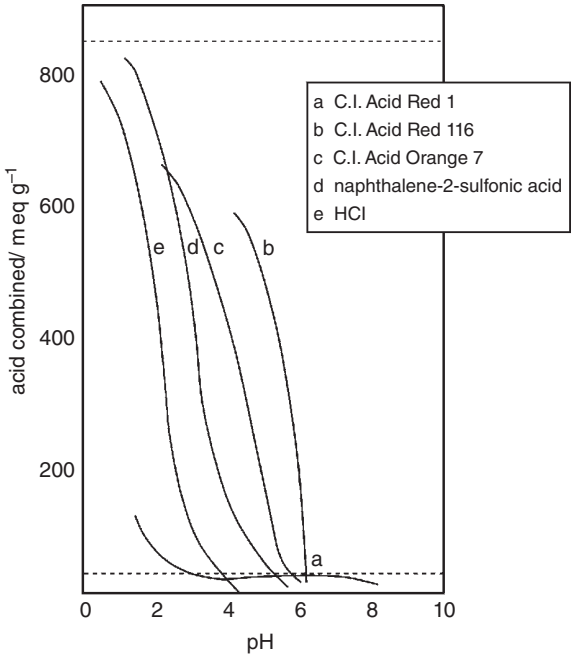

Figure 9.22 Acid titration curves for PA and wool fibres; dotted lines: respective free AEG content of wool (top) and PA (bottom). Reproduced from [230], copyright of the Society of Dyers and Colourists.

Eq. 9.1, where θ is the fractional occupation of sites in the substrate and C is the number of carboxyl groups in the fibre that for regular polyamides exceeds that of amino groups, A.

$$-\Delta\mu^{o} = RT\ln\left(\frac{\theta_{\mathrm{H}}}{1-\theta_{\mathrm{H}}}.\frac{\theta_{\mathrm{X}}}{1-\theta_{\mathrm{X}}}\right) - RT\ln\left([\mathrm{H}^{+}]_{\mathrm{s}}[\mathrm{X}^{-}]_{\mathrm{s}}\right) \tag{10.7}$$

$$\theta_{\mathrm{H}} = \frac{[\mathrm{H}^{+}]_{\mathrm{f}}}{\mathrm{C}} \quad \text{and} \quad \theta_{\mathrm{X}} = \frac{[\mathrm{X}^{-}]_{\mathrm{f}}}{\mathrm{A}} \tag{9.1}$$

Substituting the appropriate terms for θ_{H} and θ_{X} from Eq. 9.1 into Eq. 10.7 results in Eq. 9.2, which can be rewritten in the form of Eq. 9.3.

$$-\Delta\mu^{o} = RT\ln\frac{[\mathrm{H}^{+}]_{\mathrm{f}}}{\mathrm{C}-[\mathrm{H}^{+}]_{\mathrm{f}}}.\frac{[\mathrm{X}^{-}]_{\mathrm{f}}}{\mathrm{A}-[\mathrm{X}^{-}]_{\mathrm{f}}} - RT\ln\left([\mathrm{H}^{+}]_{\mathrm{s}}[\mathrm{X}^{-}]_{\mathrm{s}}\right) \tag{9.2}$$

$$K = \exp\,-\frac{\Delta\mu^{o}_{\mathrm{HX}}}{2.303RT} = \frac{[\mathrm{H}^{+}]_{\mathrm{f}}}{\mathrm{C}-[\mathrm{H}^{+}]_{\mathrm{f}}}.\frac{[\mathrm{X}^{-}]_{\mathrm{f}}}{\mathrm{A}-[\mathrm{X}^{-}]_{\mathrm{f}}}.\frac{1}{[\mathrm{H}^{+}]_{\mathrm{s}}[\mathrm{X}^{-}]_{\mathrm{s}}} \tag{9.3}$$

$[\mathrm{H}^{+}]_{\mathrm{f}}$ is the total amount of protons in the fibre. In the case of a titration curve started at the isoelectric point (i.e. when [C] = [A]), Eq. 9.4 applies in which $[\mathrm{H}^{+}]_{\mathrm{iso}}$ represents the amount of protons adsorbed by the fibre in its isoelectric state (i.e. $[\mathrm{H}^{+}]_{\mathrm{iso}}$ depends on the difference between the number of carboxylic groups, C and amino groups, A, in the substrate).

$$[\mathrm{H}^{+}]_{\mathrm{iso}} = \left([\mathrm{H}^{+}]_{\mathrm{f}} - (\mathrm{C}-\mathrm{A})\right) \tag{9.4}$$

Since, for electrical neutrality, $[\mathrm{H}^{+}]_{\mathrm{iso}} = [\mathrm{X}^{-}]_{\mathrm{f}}$, the latter being equivalent to $[\mathrm{X}^{-}]_{\mathrm{iso}}$. If HX is the only electrolyte present, when Eq. 9.4 is rewritten in the form of Eq. 9.5, it follows that, assuming $[\mathrm{H}^{+}]_{\mathrm{iso}} = [\mathrm{X}^{-}]_{\mathrm{f}}$, Eq. 9.6 applies.

$$[\mathrm{H}^{+}]_{\mathrm{f}} = \left([\mathrm{H}^{+}]_{\mathrm{iso}} + (\mathrm{C}-\mathrm{A})\right) \tag{9.5}$$

$$[\mathrm{H}^{+}]_{\mathrm{f}} = \left([\mathrm{X}^{-}]_{\mathrm{f}} + (\mathrm{C}-\mathrm{A})\right) \tag{9.6}$$

Since for electrical neutrality $[H^+]_s = [X^-]_s$ then Eq. 9.3 can be written in the form of Eq. 9.7 [178]:

$$\frac{-\Delta\mu^{o}_{HX}}{2.303\,RT} = 2\ \mathrm{pH} + \log K \tag{9.7}$$

where

$$K = \frac{\left([X^-]_f + C - A\right)\,[X^-]_f}{\left(A - [X^-]_f\right)^2} \tag{9.8}$$

Thus, a plot of log K as a function of pH should yield a straight line of slope 2, which has been obtained [178]. Taking antilogs, Eq. 9.9 results from which a plot of β versus $[X^-]_f$ provides a straight line of slope $-K^{0.5}$ and intercept A, such plots having been secured [218].

$$\beta = \frac{\left[\left([X^-]_f + C - A\right)[X^-]_f\right]^{0.5}}{[H^+]_s} = K^{0.5}\left(A - [X^-]_f\right) \tag{9.9}$$

Using this approach, values for the affinity of HCl on PA have been determined that ranged from –43.7, –45 and –45.8 kJ mol^{-1} at 18°C, 34.8°C and 55.5°C, respectively [218]. These values compare well with the average value of affinity (–44.5 kJ mol^{-1}) obtained at various points on the HCl titration curve [217].

The alternative Donnan approach described in Chapter 10 can be used to calculate the affinity of acids adsorbed by PA fibres, although greater variation in the affinity values are secured compared with those obtained assuming a Langmuir (Gilbert–Rideal) model [178, 228].

Other Models As discussed in Chapter 10, much debate has attended the applicability of the Gilbert and Rideal and Donnan models. In the case of PA fibres, several alternative models have been developed, including Peters' generalised extension [231] of his earlier Donnan model [232], Mathieson and Whewell's [233] *polyelectrolyte theory* that considered the energy required to remove adsorbed protons from the fibre and transfer these ions to the external solution against osmotic, electrostatic and affinity forces, as well as Myagkov and Paksher's *ion-exchange theory* that involved the use of appropriate dissociation constants. Iijima *et al.* [234] interpreted the titration curves of several weak acids as well as HCl on PA 6 films at 50°C in terms of a dual sorption model that involved ionised and unionised species, which were adsorbed according to a Langmuir and partition (Nernst) mechanism, respectively. The adsorption of strong acids, such as HCl and CF_3COOH, is considered to occur only by a Langmuir mechanism, the greatest contribution from a Nernst mechanism being observed for the weakest acid investigated, namely CH_3COOH [234].

9.3.1.1.3 Adsorption of Dye Anions Curves of the type shown in Figure 9.23 are typically obtained for the equilibrium adsorption of acid dyes on PA fibres as a function of pH. As the sigmoidal-shaped curves resemble those secured

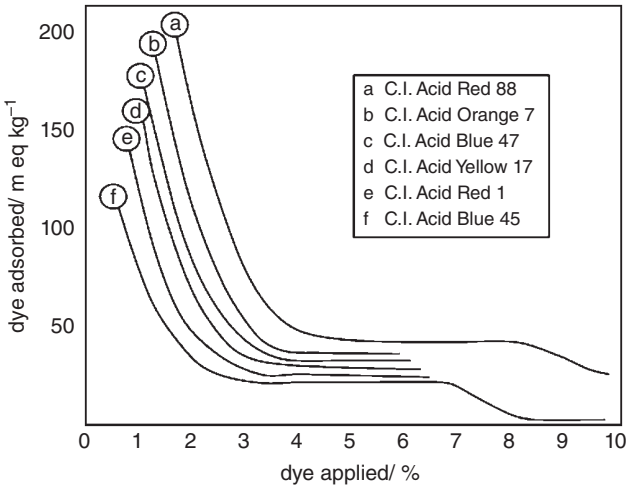

Figure 9.23 Equilibrium uptake of several non-metallised acid dyes on PA 66 as a function of pH. Reproduced from [235], copyright of the Society of Dyers and Colourists.

for the adsorption of simple inorganic acids by the substrate, they are sometimes referred to *as titration curves* of PA fibres with acid dyes.

The findings of Peters [223] and Peters *et al.* [235, 236] (Figure 9.23) for the adsorption of several mono- and di-basic, commercial and purified, non-metallised acid dyes on PA 66 reveal that the titration curves obtained for acid dyes differ from those secured for inorganic acids insofar as in the 'plateau' region of the curve in Figure 9.23, which begins at around pH 3 and corresponds to the AEG content of the fibre, extends over a wide range of pH values, whereas in the case of simple acids, this region is very narrow (Figure 9.21).

The curves shown in Figure 9.23 can be divided into three regions [223], A, B and C (Figure 9.24). In region C, at high pH values (e.g. pH 9), the carboxyl groups will be ionised and the protonated amino end groups may be non-protonated (**XVI**). In this region, it follows that adsorption of dye anions will be low. As pH decreases, dye adsorption increases as the ionisation of the carboxyl groups decreases and the amino end groups become protonated. Further dye uptake occurs with decreasing pH until it reaches a plateau region (B in Figure 9.24) that extends over several units of pH (e.g. pH 3–7) when the carboxyl groups are undissociated and the amino groups are protonated (**XIV**); in this region, dye anion adsorption attains a value that corresponds to the stoichiometric AEG content of the fibre. As pH is lowered further, in region A, a marked increase in dye uptake occurs that continues to increase with decreasing pH, apparently without limit. In this region, dye adsorption occurs in excess of the AEG content of the fibre and has been attributed to dye uptake onto protonated chain amide groups (**XIII**) and is referred to as *overdyeing*.

Thus, within the pH range ~3–7, in which dye adsorption is insensitive to pH, the equilibrium uptake of non-metallised acid dyes on PA fibres conforms to a Langmuir isotherm model [237–239] as illustrated by the results shown in Figure 9.25.

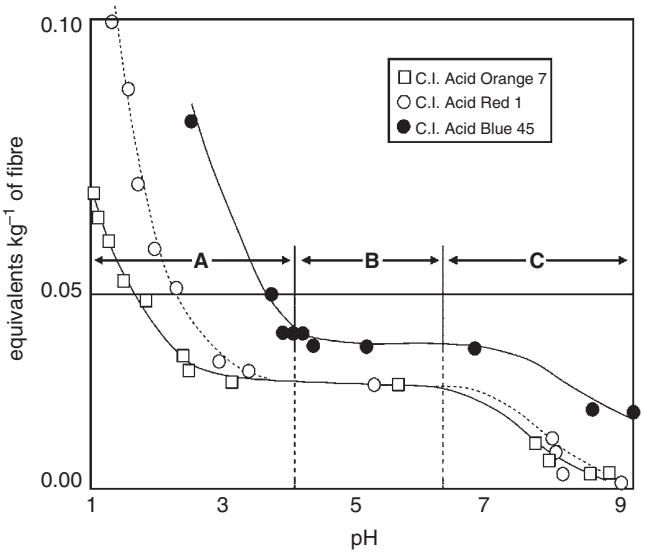

Figure 9.24 Representation of adsorption of acid dyes on PA fibres. Reproduced from [217].

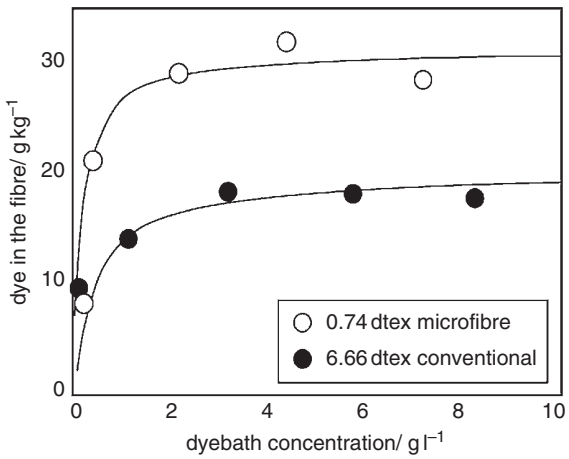

Figure 9.25 Adsorption isotherm for C.I. Acid Yellow 262 on microfibre and conventional PA 66 at 100°C and pH 5.0. Reproduced from [239], copyright of the Society of Dyers and Colourists.

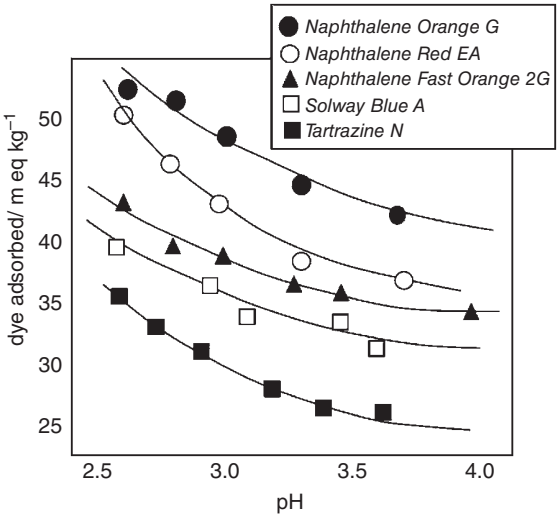

Figure 9.26 Equilibrium dye uptake as a function of pH at 75°C. Reproduced from [236], with permission from SAGE.

However, several workers [216, 240, 241] have observed deviation from the stoichiometric relationship between AEG content and equilibrium anionic dye uptake within the plateau region of the titration curves insofar as dye adsorption values were either lower or higher than the AEG content. Such findings have been attributed to the degree of sulfonation of the dye, as illustrated by the results in Figure 9.26 wherein uptake in excess of AEG was observed for the monosulfonated C.I. Acid Red 88 whilst uptake below AEG was observed in the case of the disulfonated C.I. Acid Blue 45. Atherton *et al.* [236] found that the curves for the adsorption of several dyes on PA 66 fibres within the pH range ~2.5–4.0 were not horizontal but, rather, dye uptake gradually decreased with increasing pH (Figure 9.26).

Overdyeing The adsorption of anionic dye in excess of the AEG content of the fibre, or *overdyeing*, is more important in the case of PA fibres than it is for wool because the latter fibre type contains far greater number of basic groups (Table 9.7). As discussed, three regions are discernible in the typical titration curves obtained for acid dyes on PA 66 (Figure 9.24). The positions of all three regions are clearly dye-dependent, the plateau region, B, which extends over several units of pH and corresponds to the number of amino end groups in the fibre, is often referred to as *electrostatic saturation* and dye uptake in this region is commonly assumed to corresponding to the *saturation value* of the fibre. At lower pH, in region A, dye adsorption exceeds the saturation value of the fibre and dye uptake continues to increase with decreasing pH, apparently without limit; such dye uptake greater than the AEG content of the fibre is referred to as overdyeing.

The phenomenon of overdyeing has been attributed to several causes (e.g. [9]). For example, it was suggested that overdyeing at low pH values could be attributed to dye adsorption onto new amino end groups that were created by hydrolysis of chain amide groups [240]. O'Briain and Peters [242] proposed that overdyeing occurred in two stages, namely an initial rapid uptake of dye in excess of the AEG content, followed by gradual hydrolysis resulting in an increased number of amine groups. Peters [223] suggested that the dyes combined with the amide groups, either by protonation, and subsequent adsorption of the dye anion; the absence of a maximum in dye adsorption at low pH values is thus explained by the large number of amide groups present in PA fibres. However, because overdyeing was observed at pH 4.5, where amide group protonation may not occur, Peters [178] concluded that the dyes were adsorbed in their undissociated form, a view supported by other workers [237]. Holfeld and Shepard [190] consider that, under acidic conditions, acid dyes are converted to their unionised, low aqueous solubility forms that display high solubility in PA fibre. The extent of overdyeing has been shown to be proportional to the affinity of the dye and also is related to the number of sulfonate groups in the dye, because the degree of overdyeing decreases in the order: monosulfonate > disulfonate > trisulfonate over the pH range 2–6, with tetrasulfonated dyes overdyeing only at a pH of <3 [243]. In this context, Atherton *et al.* [236] observed that in the case of PA 66 that had been acetylated to reduce its AEG content from 35 to 2.9 meq. kg^{-1}, the extent to which dye uptake was reduced followed the order: monosulfonated << disulfonated < trisulfonated [236]. It has been proposed [225], in the case of the adsorption of dye in excess of the AEG content, that the driving force for dye adsorption, $-\Delta\mu^{*o}$, can be expressed in terms of Eq. 9.10, where the gain in free energy, $-\Delta\mu^{o}$, promotes dye uptake and the gain in potential energy of the fibre surface, Π, resists dye adsorption; when $-\Delta\mu^{o} = \Pi$, then no adsorption occurs.

$$-\Delta\mu^{*o} = -\Delta\mu^{o} + \Pi \tag{9.10}$$

The generalised approach devised by Sumner [244–246], as discussed in Chapter 10, to describe the affinity of anionic dyes on PA fibres based on Donnan equilibrium theory, predicts that overdyeing can occur without invoking the formation of new sites in the fibre either as a result of ionisation of amide groups or due to fibre hydrolysis.

Measurement of Dye Affinity Relatively few attempts have been made to determine the affinity of dye anions for PA fibres directly from acid dye titration curves owing to experiment challenges that accrue from the high levels of dye exhaustion achieved [178, 217, 228]. For example, the affinity of the dibasic dyes C.I. Acid Red 13 and C.I. Acid Blue 45 was calculated using two equations based on Eq. 10.7 (see [178, 217, 228]) (i.e. assuming a Langmuir equation). Unfortunately, different values of affinity were obtained using the two approaches. In an attempt to avoid the experimental difficulties inherent in acid dye titration, desorption methods have also been used to determine affinity values. However, once again, the use of either the Gilbert–Rideal or Donnan analyses furnishes different values of affinity [178, 228].

Models of Dye Anion Adsorption on PA Fibres Both unimodal and multimodal mechanisms have been employed to describe the mechanism of adsorption of acid dyes on PA fibres, the latter approach tending to be used in the case of dye adsorption at low pH values when overdyeing can arise.

Models that describe the dyeing of PA fibres with acid dyes have been developed based on a generalised Donnan equilibrium approach, such models being applicable to other dye/fibre systems, as exemplified by the approach of Sumner [244–246] that sought to determine the affinity of anionic dyes on PA fibres (and protein fibres). The model devised by McGregor and Harris [247] assumed that no specific interactions occurred between dye anions and charged amino end groups and identified two parameters that determine ion adsorption, namely the partition coefficient, K_i and valency, z_i, of the ions, via Eq. 9.11, where λ_i is the Donnan coefficient and C^f and C^s are the concentrations of dye in the fibre and dyebath, respectively.

$$C_i^f = (\lambda_i)^z K_i C_i^s \tag{9.11}$$

Early studies revealed that the adsorption of non-metallised acid dyes (e.g. [236, 237, 248–252]) and also pre-metallised acid dyes (e.g. [251, 252]) on PA fibres could be explained in terms of a dual-mode mechanism that comprised both a Langmuir or ion-exchange mechanism and a Nernst-type mechanism. From the shape of the adsorption isotherm obtained for the monosulfonated AQ dye, C.I. Acid Blue 78 (Figure 9.27) on PA 66 fibres, Brody [237] concluded that two simultaneous and independent processes occurred, namely Langmuir adsorption via ion–ion forces and Nernst-type adsorption.

Support for this proposal was assumed from the finding that the intercept of the extrapolated linear portion of the isotherm (between 0.4 and 2.0 g l^{-1} applied dye) corresponded to dye uptake of 21 g kg^{-1}, which was close to the amount required to saturate the amino end groups. The linear portion of the isotherm was deemed to arise because of saturation of the amino end groups and was assumed to accord with the Nernst adsorption isotherm observed for disperse dyes [237]. It was proposed [253, 254] that the adsorption isotherm obtained for purified C.I. Acid Blue 182 on PA 6 film could be explained on the basis of surface diffusion incorporating three kinds of Langmuir adsorption mode, namely normal Langmuir-type adsorption, irreversible adsorption and Nernst-type adsorption. A line that fitted the experimental data well was calculated using Eq. 9.12 for this particular trimodal Langmuir adsorption approach, where

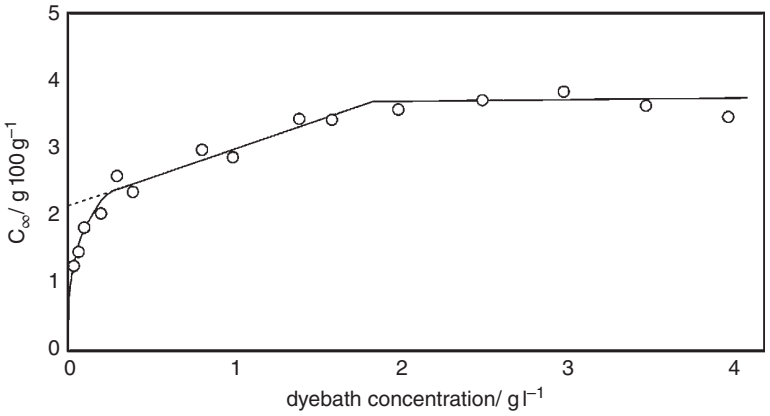

Figure 9.27 Adsorption isotherm for C.I. Acid Blue 78 on PA 66 fibres at 97°C, pH 6.0. Reproduced from [237], with permission from SAGE.

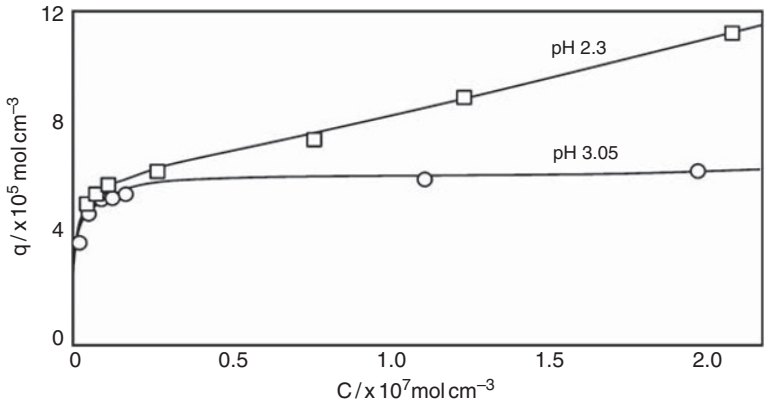

Figure 9.28 Sorption isotherm of C.I. Acid Blue 182 on PA 6 film at 80°C. Reproduced from [255], with permission from John Wiley & Sons, Inc.

q is the concentration of adsorbed dye, K_L the Langmuir-type adsorption constant, K_N the Nernst-type adsorption constant, C the concentration of dye in the pores and S the saturated concentration of adsorbed dye.

$$q = \frac{K_{L1} S_1 C}{1 + K_{L1} C} + S_2 + K_N C \tag{9.12}$$

In a subsequent study [255] of the sorption of C.I. Acid Blue 182 on PA 6 film at different pH values at 80°C, it was observed that the adsorption isotherm (Figure 9.28) could be interpreted in terms of dual-mode adsorption involving Nernst and bimodal Langmuir types (Eq. 9.13).

$$q = \frac{K_L S C}{1 + K_L C} + K_N C \tag{9.13}$$

The population of dye molecules sorbed via the former mechanism increased with decreasing pH and also, as the concentration of dye increased, dye transport within the PA film was dominated by diffusion within pores as well as surface diffusion of the adsorbed Nernst population of dye molecules. The contribution of pore and surface diffusion of the Nernst population of dye molecules increased at lower pH values.

In a study of the adsorption of purified dibasic non-metallised acid dyes coefficient in PA 6 film at 60, 70 and 80°C at pH 2.2 [256], the results were described in terms of a bimodal mechanism consisting of Nernst adsorption and ion exchange, via Eq. 9.14, where K_1 is a constant for the partition mechanism and θ_D the fractional occupation of the charged sites in the substrate.

$$C_D = K_1 C_{DS} + \frac{S\theta_D}{2} \tag{9.14}$$

The ion-exchange process is represented by Eq. 9.15, where A^- and D^{2-} are the monovalent counterion and the dye anion, respectively, K being the equilibrium constant for the ion-exchange process, which is related to θ_D by Eq. 9.16, where S is the amount of the charged sites and C_{DS} and C_{AS} are, respectively, the amounts of dye and counterion in solution.

$$2\left(-NH_3^+ \; A^-\right) + D^{2-} \rightleftharpoons \left(-NH_3^+\right)D^{2-} + 2A^- \tag{9.15}$$

$$K = \frac{C_{AS}^2}{2SC_{DS}} \frac{\theta_D}{(1-\theta_D)^2} \tag{9.16}$$

Clearly, the mechanism of the adsorption of non-metallised acid dyes on PA fibres has attracted much attention and, as the above, brief excursion into the relevant published work implies, the subject has not been entirely resolved.

9.3.1.2 Kinetics of Dyeing

The diffusion of non-metallised acid dyes in PA fibres is markedly concentration-dependent (e.g. [187, 257, 258]), as illustrated by the sigmoidal-shaped concentration–distance profiles obtained for C.I. Acid Red 18 in PA 66 film

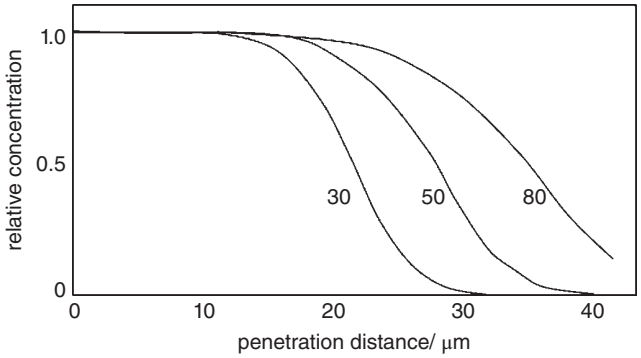

Figure 9.29 Diffusion of C.I. Acid Red 18 in PA 66 film. Reproduced from [259], copyright of the Society of Dyers and Colourists.

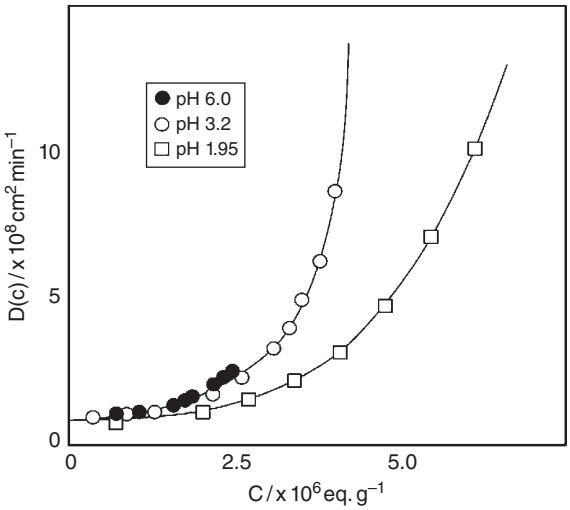

Figure 9.30 Relation between real (measured) diffusion coefficient and concentration for C.I. Acid Red 18 in PA 66 film at 60°C. Reproduced from [260], with permission from the Royal Society of Chemistry.

(Figure 9.29) and the concentration-dependence of the real (measured) diffusion coefficient, $D(c)$, calculated from analysis of such curves using Eq. 9.17, where $\eta = x/2t^{1/2}$ [178], in the case of the trisulfonated dye C.I. Acid Red 18 in PA 66 film under conditions of surface saturation (Figure 9.30) [187, 257].

$$D(c) = -2\frac{d\eta}{dC}\int_0^{C_1} \eta \, dC \tag{9.17}$$

The observed concentration-dependence of diffusion coefficient has been explained in terms of the nature of the interactions that occur between the dyes and the protonated amino end group sites in the substrate [9]. Initial dye uptake can be envisaged to occur on protonated amino end groups sites located at the surface of the fibre. For subsequent dye adsorption to occur, either additional dye molecules must penetrate the dyed surface and diffuse to dye sites within the fibre interior or adsorbed dye molecules must desorb from their original position at the surface and diffuse within the fibre interior, becoming adsorbed onto other protonated AEG's. These processes will depend on factors such as the availability/accessibility of dye sites, dye–fibre affinity, temperature and concentration gradient. When dyeing commences, dye uptake can be expected to be high, owing to the high availability and accessibility of protonated AEG sites at the fibre surface and the high dye concentration gradient across the fibre; this is reflected in the characteristic high strike of non-metallised acid dyes on PA fibres. However, such a situation likely results in a large proportion of dye molecules being immobilised at the fibre surface, resulting in low diffusion coefficient. In the later stages of dyeing, as fibre saturation is approached, the number of adsorbing dye molecules falls, as does concentration gradient, and the number of immobile dye molecules also reduces, so diffusion coefficient increases. The significance of amino end groups in terms of dye diffusion is demonstrated by the observations [261, 262] that the rate of uptake of non-metallised acid dyes is proportional to the AEG content of the fibre.

Both an increase in dyeing pH (Figure 9.31a) [187] and added electrolyte (Figure 9.31b) [187] reduce the concentration-dependence of dye diffusion, as a consequence of reduced dye adsorption on the fibre.

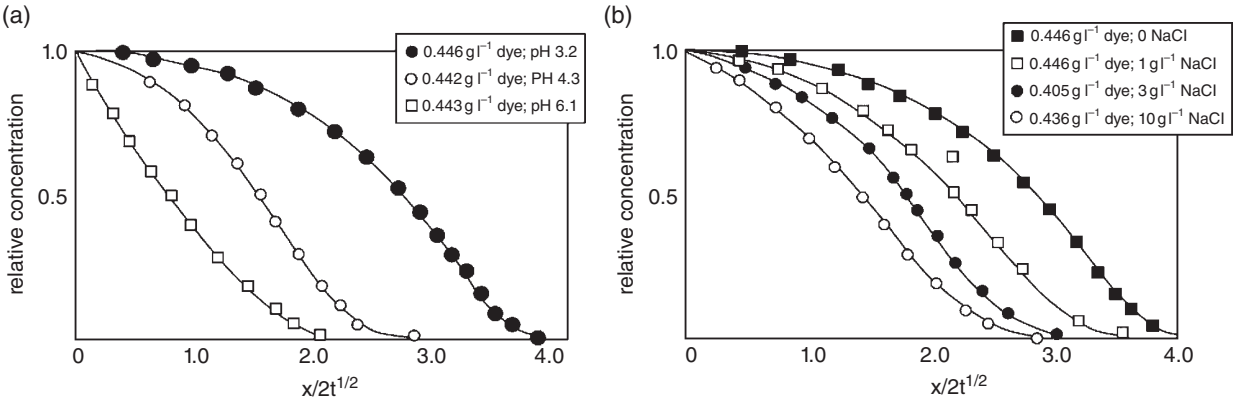

Figure 9.31 Concentration profiles for C.I. Acid Red 18 as a function of (a) pH and (b) NaCl concentration on PA 66 film at 60°C. Reproduced from [187], copyright of the Society of Dyers and Colourists.

At very low pH, the change in $D(c)$ as a function of dye concentration is more gradual at low pH values, as demonstrated by the results obtained at pH 1.95 (Figure 9.30). Under such conditions, when overdyeing occurs, acid dye diffusion is concentration-independent [237, 260]. It is proposed that the diffusion of dye that is adsorbed onto amide groups conforms approximately to Fick's law (i.e. the diffusion coefficient is independent of dye concentration) whereas in the case of dye that is adsorbed onto the amino end groups, diffusion coefficient increases rapidly as saturation of the AEG sites progresses (i.e. the diffusion coefficient is concentration-dependent) [260].

The concentration-dependent diffusional behaviour of non-metallised acid dyes in PA substrates has been interpreted in terms of both *unimodal* and *multimodal* adsorption models. According to the former approach [187], the fibre is assumed to comprise water-filled pores within which the dye anions diffuse and are instantaneously adsorbed on the pore surfaces. When the substrate is immersed in an acidic dyebath, the acid is adsorbed very rapidly, which is then followed by the more slowly diffusing dye anions that displace the adsorbed acid anions so that electrical neutrality is preserved. As the inorganic anions are assumed to have negligible substantivity, they are regarded as simply being dissolved within the pore liquid; in contrast, the dye ions are strongly adsorbed by means of a Langmuir isotherm. Atherton and Peters [263] proposed that acid dye diffusion in PA fibres is governed not only by the dye concentration gradient across the substrate but also by the number of dye sites that are available and accessible in the fibre, because of the significance of AEG content on dye diffusion. In the latter case, it can be assumed that the driving force for diffusion will be some fraction of the occupied dye sites in the fibre, θ, and those unoccupied $(1-\theta)$, the most logical quantity being the ratio of these two quantities, namely $\theta/(1-\theta)$, this being the activity of a monobasic dye. Thus, it was suggested [263] that *concentration gradient* (dC/dx) as the driving force for diffusion that is normally employed in Fick's first law could be replaced by the gradient of chemical potential of the dye anion (i.e. *activity gradient*), which resulted in two equations that described the variation of $D(c)$ with θ (Eqs. 9.18 and 9.19).

$$D(c) = \frac{D_o}{(1-\theta)^2} \quad \text{(activity gradient model)} \tag{9.18}$$

$$D(c) = \frac{D_o}{(1-\theta)} \quad \text{(chemical potential gradient model)} \tag{9.19}$$

Whilst neither Eq. 9.18 nor 9.19 provided exact representations of the experimentally determined diffusional behaviour of C.I. Acid Red 18 in PA 66 [178], Eq. 9.19 provided a better description of the variation of diffusion coefficient with θ (Figure 9.32).

Because not all the amino end groups may be accessible and therefore the relationship between amino end groups in the fibre and the dye anions may likely not be stoichiometric, replacing the dye site occupation term θ in Eqs. 9.18 and 9.19 with an accessibility factor $\alpha\theta$, where $\alpha\theta < 1$, improved agreement with experimentally derived results [187]. An equation based on the assumption that an electrical potential gradient arises when the dye anion exchanges with an adsorbed Cl^- ion also provided improved agreement with practical results [259].

Several workers have interpreted the concentration-dependent diffusional behaviour of non-metallised acid dyes in PA fibres in terms of a multimodal adsorption mechanism. For example, Komiyama and Iijima [250] described the concentration-dependent diffusion of several monoanionic dyes in PA fibres on the assumption that a dynamic equilibrium existed between two thermodynamically distinct populations of dye molecules, the adsorption of the two dye types, namely *adsorbed* and *dissolved*, occurring by means of Langmuir and Nernst mechanisms, respectively. Eq. 9.20

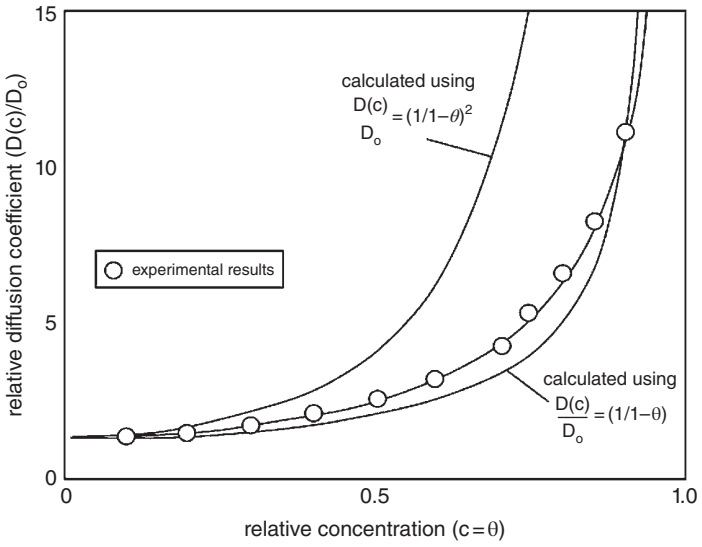

Figure 9.32 Test of thermodynamic equations for C.I. Acid Red 18 in PA 66. Reproduced from [259], copyright of the Society of Dyers and Colourists.

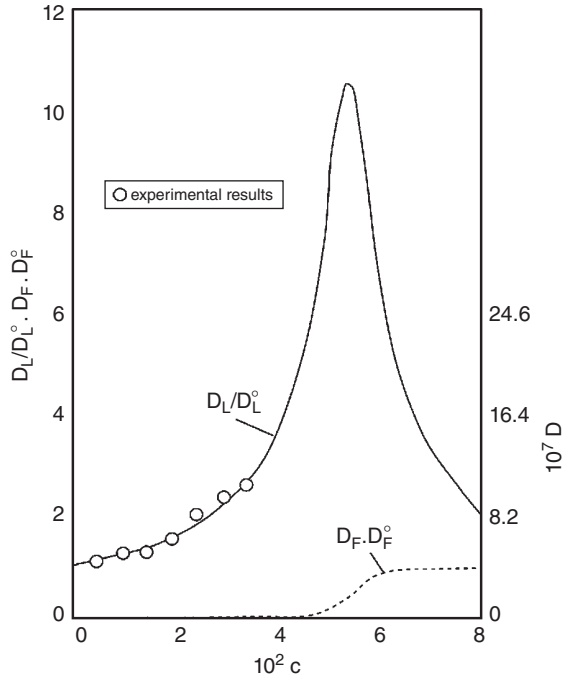

Figure 9.33 Experimental (points) and calculated diffusion coefficients as a function of dye concentration for C.I. Acid Orange 7 in PA 6 film, the right ordinate refers to experimental and the left calculated values. Reproduced from [250], with permission from John Wiley & Sons, Inc.

was derived to describe this multimodal adsorption process where D_L^o and D_P^o represent the contributions of the respective Langmuir and partition species to the apparent diffusion coefficient, $D(c)$, K_P being the partition coefficient of the dissolved dye molecules, K_L that of the adsorbed dye molecules and S the saturation value of the fibre (= AEG content).

$$D(c) = RT\left[D_L^o \frac{\alpha(1-\theta)}{\alpha(1-\theta)^2+1} + D_P^o \frac{1}{\alpha(1-\theta)^2+1}\right] \tag{9.20}$$

Figure 9.33 shows that, in the case of the diffusion of C.I. Acid Orange 7 in PA 6 film, Eq. 9.20 predicts that $D(c)$ increases gradually at first and steeply thereafter as a function of increasing saturation of the amino end groups, reaching a maximum value corresponding the AEG content of the film. In terms of the concentration-dependence of dye diffusion, the behaviour of the adsorbed species, via D_L, is of prime significance.

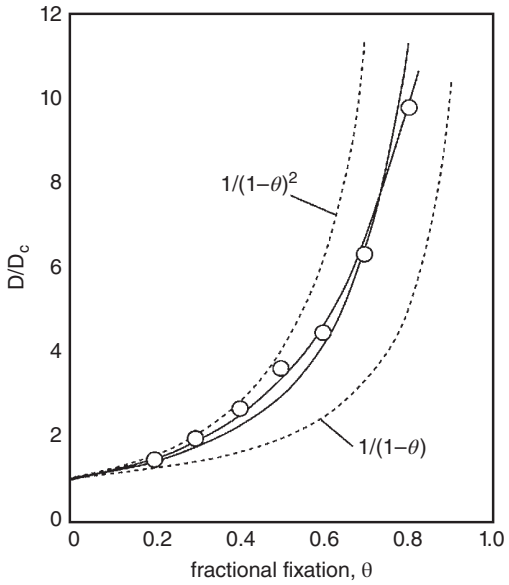

Figure 9.34 Variation in relative diffusion coefficient with relative concentration compared with theoretical predictions for C.I. Acid Red 18 on PA 66 film; $1/(1-\theta)$ relates to Eq. 9.10 and $1/(1-\theta)^2$ to Eq. 9.9. Reproduced from [266], copyright of the Society of Dyers and Colourists.

Such a bimodal approach has subsequently been applied to the diffusion of disulfonated direct dyes [264], a trisulfonated acid dye in the presence of NaCl [249], acid dyes and food dyes [265], as well as mono-, di- and tri-sulfonated non-metallised acid dyes [253] within PA 6.

Sada *et al.* [266] proposed that acid dye diffusion in PA could be described using a parallel-transport model that comprised both surface and pore diffusion accompanied by simultaneous bimodal Langmuir adsorption, the latter taking into account one site being more physically active than another. The concentration-dependence of the diffusion coefficient determined using this model was compared with corresponding experimentally measured data obtained by other investigators. In this context, when the results obtained by Hopper *et al.* [187] were evaluated, the parallel-transport model provided a better description of the variation of diffusion coefficient with θ compared to either Eq. 9.18 or 9.19, for the diffusion of C.I. Acid Red 18 in PA 66 film (Figure 9.40), in which the unbroken line is the curve obtained using Eq. 9.21. The low correspondence with experimental data at low fractional fixation values (Figure 9.34) was attributed to pore diffusion, in which case, the concentration dependence of the diffusion coefficient was described by pore diffusion with simultaneous bimodal Langmuir adsorption, as given by Eq. 9.22, this being shown by the remaining line in Figure 9.34, which provides good agreement with experimental data over a wide range of fractional fixation values.

$$D = \frac{\left(\frac{z_1 z_2}{K_1 S_1}\right) D_P + z_2 (1-\theta_1) D_1^o + z_1 \left(\frac{K_2 S_2}{K_1 S_1}\right) D_2^o}{z_2 (1-\theta_1)^2 + z_1 \left(\frac{K_2 S_2}{K_1 S_1}\right)} \tag{9.21}$$

$$D = \frac{\left(\frac{z_1 z_2}{K_1 S_1}\right) D_P}{z_2 (1-\theta_1)^2 + z_1 \left(\frac{K_2 S_2}{K_1 S_1}\right)} \tag{9.22}$$

In a subsequent study, it was found that the concentration-dependent diffusion of C.I. Acid Blue 182 in PA 6 film was governed by surface diffusion that incorporated three kinds of Langmuir adsorption modes, namely normal Langmuir-type adsorption, irreversible adsorption and Nernst-type adsorption [268]. These authors also observed for this particular dye that at high concentrations, under the dyeing conditions used (80°C; pH 2.1), true dye adsorption equilibrium was not achieved immediately within the PA 6 film but, rather, a quasi-equilibrium was attained after ~2.5 h after which dyes gradually diffused into regions of low dye penetration; true equilibrium was achieved after some 30 h (Figure 9.35).

It was therefore proposed [268] that the substrate comprises two interconnected regions, namely one that is available for rapid dye penetration and another that displays low penetrative character and which is created by the slow relaxation of the polymer. It was argued that when dye molecules penetrate the PA 6 film, the substrate undergoes structural

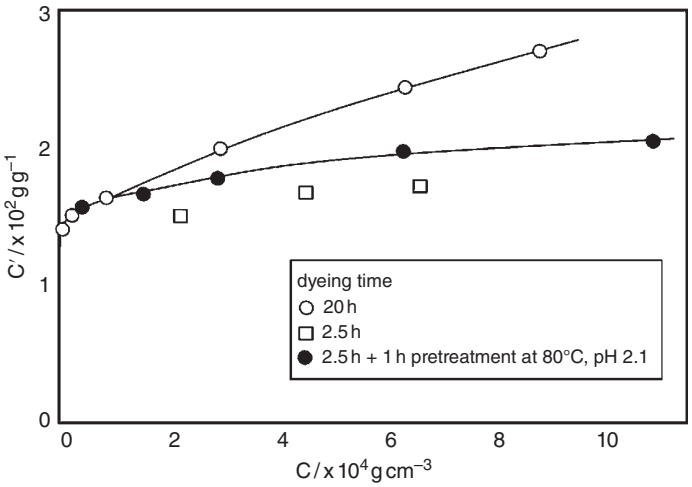

Figure 9.35 Relationship between concentration of C.I. Acid Blue 182 in solution and in PA 6 film for various dyeing times. Reproduced from [268], copyright of the Society of Dyers and Colourists.

rearrangement so as to accommodate the dye molecules. Such a process, which involves segmental chain movement, was considered as not being instantaneous but, rather, occurred gradually. It was suggested [254] that such relaxation processes increase only the amount of dye adsorbed according to a Nernst mechanism and do not affect dye uptake that accords with Langmuir adsorption. Furthermore, it was found [254] that the concentration-dependence of the diffusion of C.I. Acid Blue 182 in PA 6 film could be described in terms of surface diffusion involving one partition (Nernst) and two Langmuir adsorption mechanisms, except in the case of high applied dye concentrations, for which the diffusional behaviour of the dye could be described in terms of two Langmuir-type adsorption equilibria that were established throughout the substrate, together with a pseudo-equilibrium partition (Nernst) type adsorption. Subsequent studies [255] revealed that, in the case of the diffusion of C.I. Acid Blue 182 in PA 6 film being described in terms of parallel diffusion involving Nernst and bimodal Langmuir types, the population of dye molecules sorbed via the Nernst mechanism increased with decreasing pH and also, as the concentration of dye increased, dye transport within the PA film was dominated by diffusion within pores as well as surface diffusion of the adsorbed Nernst population of dye molecules. The contribution of pore and surface diffusion of the Nernst population of dye molecules increased at lower pH values.

The diffusion of purified, dibasic, non-metallised acid dyes in PA 6 film at 60, 70 and 80°C and at pH 2.2 [256] was interpreted in terms of a bimodal mechanism consisting of Nernst adsorption and ion-exchange, via Eq. 9.23, where D_1 and D_2 are the apparent diffusion coefficients of the partition and ion-exchange species, respectively, D_{T1} and D_{T2} the thermodynamic diffusion coefficients and θ_D the fractional occupation of the charged sites in the substrate. β is given by Eq. 9.24, where K is the equilibrium constant of the ion-exchange process, K_1 a constant for the partition mechanism, S the concentration of the charged sites and C_{AS} the concentration of counterions in solution.

$$D(c) = D_1 + D_2 = \left[\frac{D_{T1}}{\beta(1-\theta_D)^2} + D_{T2}\right]\left[\frac{1+\theta_D}{1-\theta_D + \dfrac{1+\theta_D}{\beta(1-\theta_D)^2}}\right] \tag{9.23}$$

$$\beta = \frac{K}{K_1}\left(\frac{S}{C_{AS}}\right)^2 \tag{9.24}$$

As discussed earlier, fibre drawing enhances the orientation of the polymer chains, which results in increased alignment of the non-crystalline regions and increased crystallinity, to extents that vary for different types of fibre. The effects of heat setting and steam setting on PA fibres have been extensively studied (e.g. [182, 269–281]). For example, when PA 6 and PA 66 yarns were subjected to dry heat setting, the rate of dyeing using C.I. Direct Blue 71 initially fell and then increased with increasing heat-setting temperature [182].

Although both dry heat and saturated steam increase the density of the fibre and therefore the degree of crystallinity, which would suggest a gradual decrease in dye accessibility, the orientation of the crystalline units remains virtually unchanged [182, 274, 279]. Such a dichotomy can be explained by assuming that two opposing processes might occur, namely one in which the accessible void space between the crystallites is reduced and thereby the tortuosity of the voids increases, which will serve to reduce dye accessibility, and one in which the amount of void space

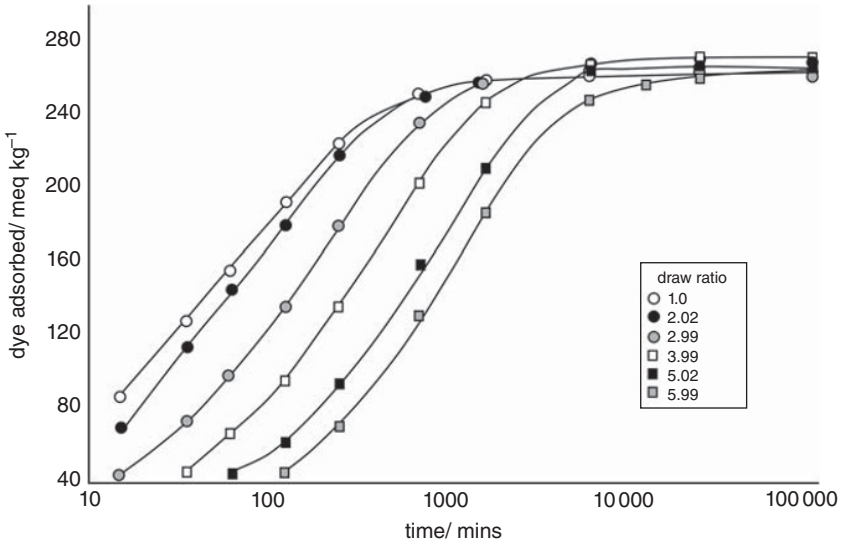

Figure 9.36 Rate of dyeing curves for C.I. Acid Orange 7 on PA 66 at 60°C. Reproduced from [285], with permission from SAGE.

increases as a result of increased perfection of the crystallites, which will result in increased dye accessibility [282]. Steam setting increases the rate of dyeing PA fibres compared to untreated fibre, which, in turn, displays higher dyeing rates than PA fibre that has been dry heat set. Such differences in dyeing rate are considered to arise from differences in the packing of the polymer chains within the amorphous regions of the substrate [283]. The role of the extensive H-bonded structure of the polymer seems the key, and in the presence of steam, the chains may be more mobile and form a more open network than when heat setting is undertaken dry [283]. In the case of PA 66, whilst drawing has little effect on equilibrium dye uptake, it dramatically reduces the rate of dyeing [284] as shown by the results displayed in Figure 9.36.

The aforementioned short discussion of some of the published work relating to the concentration-dependent, diffusional behaviour of non-metallised acid dyes in PA fibres clearly shows that the subject has attracted much attention and, as mentioned earlier in the case of the mechanism of adsorption of the dyes on the substrate, the precise nature of the processes involved has not been entirely resolved.

9.3.2 Pre-metallised Acid Dyes (Aka Metal Complex Dyes)

The essential features of the chemistry and properties of this type of dye, which was developed to overcome the inherent disadvantages of using *mordant* dyes on wool (i.e. fibre tendering under prolonged dyeing times and problematic colour matching), are discussed in Chapter 10. In the *Colour Index* [212], metal complex dyes are included in the *Acid Dye* application classification, and therefore the dyes are also referred to as *pre-metallised acid dyes*.

9.3.2.1 General Application Properties [9, 180]

Only certain 1 : 1 pre-metallised acid dyes are utilised in PA fibre dyeing because many examples of this dye type display generally low saturation values and poor coverage of barré. This type of dye is commonly applied to PA fibres at the commercial boil in the pH region 4–6, in the absence of levelling agents, the ensuing moderately bright dyeings displaying good wet fastness and very good light fastness. The generally lower aqueous solubility of 1 : 2 metal complex dyes results in typically greater build-up than their 1 : 1 counterparts on PA fibres. Such dyes are applied in the pH range 5–8, depending on the dye type, in the presence of levelling agents at temperatures up to 110°C, the resulting dyeings, which may be aftertreated with syntans [286–290], displaying characteristically high all-round fastness.

9.3.2.2 Mechanism of Adsorption

The mechanism of dyeing PA fibres with metal complex dyes has received surprisingly little attention. Back and Zollinger [252] studied the equilibrium uptake of a weakly polar 1 : 2 metal complex dye on PA 66 (Figure 9.37) and, as the dye was also adsorbed onto acetylated PA 66, it was proposed that dye uptake occurred, simultaneously, via two mutually independent mechanisms, namely a Langmuir process at the protonated amino end groups and a solution

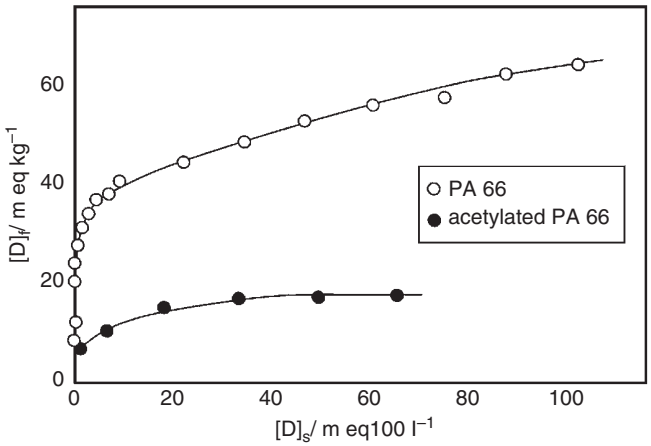

Figure 9.37 Equilibrium adsorption of weakly polar 1 : 2 metal complex dye on PA 66 and acetylated PA 66. Reproduced from [252], with permission from Wiley-VCH Verlag GmbH.

(i.e. partition or Nernst) mechanism; Langmuir adsorption accorded with the AEG content of the material. Subsequent studies [251] revealed that the partition mechanism, which involved adsorption of the undissociated dye on the amide group, predominated with increasing acidity. Comparative isotherms undertaken using PA 66, PA 68 and PA 610 showed that the contribution of the partition mechanism decreased in the order: PA 66 > PA 68 > PA 610.

In a study using a series of 1 : 2 metal complex dyes of varying hydrophobic/hydrophilic balance, it was found that the adsorption isotherms of the more hydrophilic dyes accorded with a Langmuir mechanism and the hydrophobic dyes tended to yield uptake in excess of the AEG content of the substrate [291].

9.3.3 Aftertreatment

As mentioned, despite the popularity of non-metallised acid dyes on PA fibres, the fastness to wet treatments of dyeings often leaves much to be desired, which necessitates the use of an aftertreatment with either natural or synthetic tanning agents in order to secure adequate levels of wet fastness. Although 1 : 2 pre-metallised acid dyes generally exhibit superior wet fastness on PA fibres to that of their non-metallised acid dye counterparts, an aftertreatment of substrates dyed with 1 : 2 metal-complex dyes with a *natural tanning agent* or *synthetic tanning agent* is often employed in order to secure highest levels of wet fastness [9]. The aftertreatment of dyed PA fibres has been discussed thoroughly (e.g. [9, 292] and the references therein).

9.3.3.1 Natural Tanning Agents

Natural vegetable tannin extracts, which are obtained from a wide range of plant sources, have been used for several thousand years to preserve animal skins by the process of *tanning* (e.g. [293–295]). Such extracts contain various amorphous materials that include large molar mass polyphenolic *tannins* and less complex, lower molar mass *non-tannin* materials such as gums and flavones. Natural tannins are classified as *condensed (non-hydrolysable) tannins* and *hydrolysable* (aka *pyrogallol*) *tannins*, the latter being of two types, namely *gallotannins* (e.g. tannic acid **XVII**) and *ellagitannins* (e.g. chestnut).

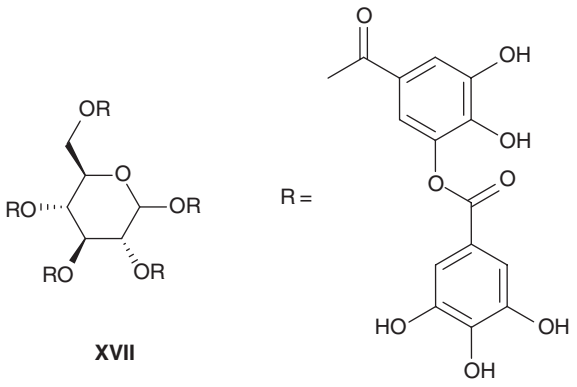

XVII

Natural tannins are water-soluble phenolic compounds that undergo reactions typical of phenols, notably the chelation of metal ions, a characteristic that has been greatly utilised from a dyeing perspective. The early textile uses of natural tannins included dyeing cotton with dyewoods (e.g. Logwood Black), the tanning agent being used to insolubilise the metallic mordant employed (e.g. $CuSO_4$) by means of the formation of a metal tannate complex. Perhaps the most famous textile use of natural tanning agents was that devised by Perkin and Pullar [296, 297] to enhance the inherent low substantivity and fastness properties of Mauve on cotton, by mordanting the fibre with tannin, which had been insolubilsed using stannous salts; in 1882, Dale found that pre-mordanting with the *full backtan* (tannin/*potassium antimony tartrate*, aka *tartar emetic*) was also successful [296]. Tannins were also used to replace the mass loss incurred during the processing of silk, metal salts of Sn and Sb being used to improve the fatness of the natural tanning agent.

More recent applications of natural tannins in dyeing include the application of tannic acid both as *stain-resistant treatments* for PA carpets and, of relevance to this particular discussion, as aftertreatments to improve the wet fastness of acid dyes on PA substrates. In the latter context, the *full backtan* aftertreatment that was devised in the 1950s involved consecutive treatments with tannic acid, potassium antimony tartrate and stannous chloride [298], the more common, simplified version omitting the use of the tin salt. The mechanism by which the two-stage full backtan improves the wet fastness of acid dyes on PA fibres involves adsorption of the high molar mass acid onto protonated amino end groups in the fibre. The subsequent application of potassium antimony tartrate serves to insolubilise the tannin, which results in the formation of a sparingly water-soluble, antimony tannate complex located at the periphery of the dyed fibre, which resists diffusion of the dye out of the substrate during washing (e.g. [9, 292, 298]). The precise nature of the antimony tannate complex has not been elucidated.

However, despite the significant improvements that the full backtan imparts to the wet fastness properties of PA fibres dyed with acid dyes, the process suffers from various inherent disadvantages [9], namely acute toxicity of potassium antimony tartrate, deterioration of fabric handle, reduction of light fastness and shade change. Various methods have been devised to overcome these disadvantages. For example, modified full backtan aftertreatments have been developed that involve the sequential application of tannic acid and a tin sulfate-based product [290, 299, 300] as well as ferrous sulfate [301], wherein the Sn or Fe salts form a metal tannate complex with the tannic acid, which thus circumvents the use of the toxic potassium antimony tartrate. Subsequently, it was shown that the toxic antimony salt can be replaced by protease enzymes [302–304] and, also, that the use of tannic acid alone secures marked improvements in wet fastness [305].

9.3.3.2 Synthetic Tanning Agents

Despite the ability of the full backtan to impart significant improvement to the wet fastness properties of PA fibres that have been dyed with acid dyes, the previously recounted inherent disadvantages associated with its use [9] have resulted in synthetic tanning agents (*syntans*) mostly replacing the natural product-based aftertreatment. Although synthetic tanning agents were originally developed as alternatives for natural tannins used in leather manufacture (e.g. [9]), syntans were subsequently developed specifically to improve the wet fastness properties of acid-dyed PA fibres. Such compounds are of diverse composition, typically being water-soluble, formaldehyde polycondensates of anionic, formaldehyde polycondensates of sulfonated dihydroxydiphenylsulfones [9, 292, 306–308]. Syntans offer the advantage of a single-stage application process compared to the common, two-bath, two-stage, full backtan process and do not suffer from the disadvantages displayed by their natural counterpart. Typically, syntans are applied to dyed PA fibres under acidic conditions for ~30 min at 70°C in the case of PA 6 or 95°C for dyed PA 66 [9].

It is considered that syntans are adsorbed at the periphery of the dyed PA fibre and that this peripheral 'layer' of large molar mass syntan molecules reduces the tendency of the acid dye to diffuse out of the fibre during washing.

The contribution that ion–ion forces make towards syntan-fibre substantivity has been shown by the findings [309, 310] that the uptake of two syntans onto PA 66 increased with decreasing pH over the region pH 2–7. The fact that syntan uptake increased with decreasing liquor ratio was attributed to aggregation of the syntan that occurred by virtue of various polar and non-polar forces of interaction [310]. The sorption of a commercial syntan onto PA 6 fibres was found to follow a Freundlich model [311], although a dual sorption mechanism comprising partition (Nernst) and Langmuir models fitted the isotherms obtained for a commercial syntan on PA 66 [312]. In contrast, a BET mechanism has been observed in the cases of commercial agents on PA 66 [309] as well as both PA 6 and PA 66 [313] and also on wool [314, 315], indicating that syntan uptake occurs initially by the formation of a monolayer followed by multilayer adsorption of syntan molecules at the PA surface.

Since an aftertreatment with a syntan is not always as effective as the full backtan in improving the wet fastness of acid dyes on PA fibres, several approaches have been devised to enhance the effectiveness of syntans. For example, it has been shown that the effectiveness of syntans in improving the wash fastness of both non-metallised acid dyes

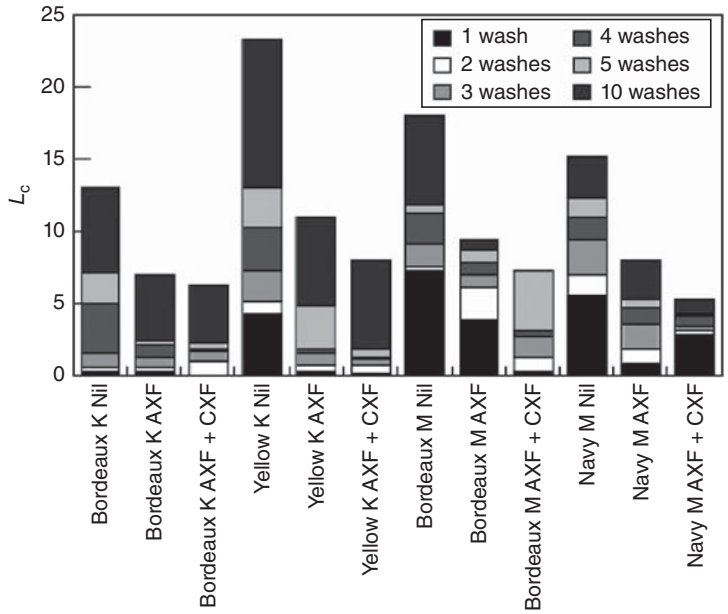

Figure 9.38 Cumulative effect of repeated wash fastness testing at 60°C on the loss of colour strength, L_c/%, of four 1 : 2 pre-metallised acid dyes on PA 66 fabric; AXF = syntan; AXF + CXF = syntan/cationic agent. Reproduced from [287], copyright of the Society of Dyers and Colourists.

[316, 317] as well as pre-metallised acid dyes [286–288] on PA 66 fibres can be enhanced by the subsequent application of a selected cationic agent (Figure 9.38). It is considered [9, 316] that this two-stage aftertreatment process results in the formation of a low water-solubility, large molecular size complex between the cationic compound and the anionic syntan within the dyed substrate.

9.4 Disperse Dyes

The good build-up and excellent migration power of disperse dyes on PA fibres together with their ability to cover fibre irregularities were recognised shortly after the commercial introduction of the fibre (e.g. [191, 208, 318–320]). In general, disperse dyes on PA fibres display moderate fastness to wet treatment and selected disperse dyes are recommended for dyeing PA fibres, typically at 98°C (although temperatures upto 110 or 120°C can be used for PA 6 and PA 66, respectively) at pH 6–7 in the presence of anionic levelling agents.

It is generally accepted that the mechanism of the adsorption of disperse dyes on PA fibres and the diffusional behaviour of this class of dye within PA fibres accords with that described in detail for PES fibres, recounted in Chapter 8.

9.5 Mordant Dyes

The chemistry and properties of this dye class are discussed in Chapter 10. In essence, mordant dyes resemble non-metallised acid dyes structurally in that the low molar mass, anionic colorants contain sulfonate and/or carboxyl groups. However, mordant dyes also contain nucleophilic groups (—NH_2, —OH, etc.), which enable them to form a coordination complex with a metal ion (commonly Cr) *in situ* within the fibre. In the case of PA fibres, the *afterchrome* dyeing method (i.e. the mordant, commonly $K_2Cr_2O_7$ or $Na_2Cr_2O_7$ is applied after the dye) is mostly employed. The dyes cover physical fibre irregularities well but are sensitive to chemical variations, and yield mostly dull shades of good all-round fastness on PA fibres.

Early studies [208, 321] of the dyeing of PA fibres with mordant dyes established that neither the *pre-chrome* nor the *metachrome* application methods were appropriate owing to inadequate mordant dye–Cr complexation [208] and that the afterchrome method was most suitable. It was observed that, when compared to the mordant dyeing of wool, greater amounts of dichromate [191, 208] and lower pH values [191] were required in the case of PA fibres. Also, the afterchrome method can result in reduced fabric strength and incomplete Cr–dye complexation for some dyes [321].

Furthermore, as PA fibres, unlike wool, cannot reduce Cr(VI) to Cr(III) during the chroming stage, reducing agents (e.g. $Na_2S_2O_3$) are necessary to achieve complete reduction of dichromate [321]. Elevated dyeing temperatures can also be used without recourse to a reducing agent [322]. The equilibrium uptake of dichromate on PA 66 fibres at pH 2.8–3 was found to correspond to the AEG content of the substrate.

It can be considered that before their complexation with Cr salts, the mechanism of adsorption and the diffusional behaviour of mordant dyes on PA fibres accords with that described for non-metallised acid dyes.

9.6 Direct Dyes

The characteristics of this dye class have been discussed in Chapter 7. From the perspective of PA fibre dyeing, direct dyes resemble non-metallised acid dyes insofar as the, typically large molar mass, azo dyes contain sulfonate groups. Owing to their characteristic large molecular size, the dyes tend to highlight physical irregularities, are sensitive to chemical variations in the PA fibres and display low migration characteristics. Selected members of the class, applied under weakly acidic conditions (∼pH 4–6), are used to provide economically attractive dyeings in particular hues; an aftertreatment with a syntan improves the wet fastness of the dyeings [9, 323].

The mechanism of adsorption and the diffusional behaviour of this dye class on PA fibres can be considered to resemble that of non-metallised acid dyes.

The dyeing of PA fibres with direct dyes was described shortly after the commercial introduction of the fibre (e.g. [191, 208, 211, 324]). Both the rate and extent of dye uptake is pH-dependent (Figure 9.39) and the diffusional behaviour of the dyes is similar to that of acid dyes in the substrate [264].

9.7 Reactive Dyes

From the perspective of PA fibres, a distinction can be made between anionic and disperse reactive dyes [9].

In the absence of covalent bond formation with the substrate, the mechanism of adsorption and the diffusional behaviour of anionic reactive dyes and disperse reactive dyes on PA fibres, can be considered to accord with that described for non-metallised acid dyes and disperse dyes, respectively.

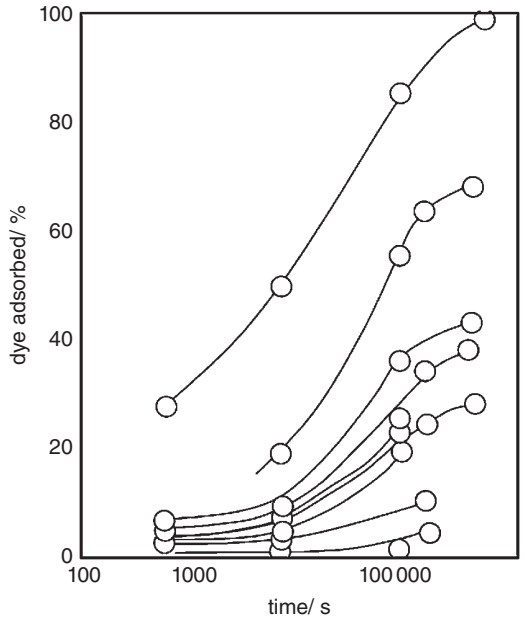

Figure 9.39 Effect of pH on rate and extent of dye uptake of *Chlorazol Fast Orange AG* on PA 66 from the top of plot: pH 1.2; 2.8; 3.3; 3.9; 4.2; 4.8; 5.6; 6.4; 7.4. Reproduced from [220], copyright of the Society of Dyers and Colourists.

9.7.1 Anionic Reactive Dyes

Although the chemistry and application of anionic reactive dyes have received enormous interest over the past 60 or so years since the commercial introduction of this dye class for cellulosic fibres in 1956, this prodigious research output has been focused, overwhelmingly, on cellulosic fibres. Considerably less attention has attended reactive dyes intended for use on protein fibres, notably wool, and even less consideration has concerned reactive dyes for PA fibres. This situation is reflected in the facts that, when compared to cellulosic fibres, not only have fewer reactive dye ranges been specifically marketed for use on wool and even fewer for use on PA fibres but also fewer publications have appeared that concern the reactive dyeing of wool and only a very small number of articles relate to the dyeing of PA fibres with reactive dyes. Furthermore, studies of reactive dyes on PA fibres have mostly concerned reactive dyes marketed for cellulosic and wool fibres.

Conventional reactive dyes intended for use on cellulosic fibres and wool fibres are typically polysulfonated chromogens that contain reactive centres capable of forming covalent bonds with nucleophilic groups in the substrates. Selected examples of such dyes can be applied to PA fibres from weakly acidic dyebaths (pH 4–6) in the presence of a levelling agent, and covalent bonds are formed between the dyes and the amino end groups (i.e. $-NH_2$) in the fibre. As a result of such covalent bonding, reactive dyed PA fibres can display high fastness to wet treatments. However, the extent of fixation achieved for the dyes, which characteristically are very sensitive to fibre irregularities, is limited by the number of accessible terminal amino end groups, which generally results in only pale/moderate depths of shade being achievable in the case of regular AEG PA fibres, although deeper shades are possible in the case of deep-dye variants, as discussed later. At higher depths of shade, the anionic dyes are present within the substrate as, essentially, acid dyes that are not covalently attached to the substrate, and therefore the wet fastness of such heavy depth dyeings leaves much to be desired.

The reasons for the typically low depths of shade achieved on PA fibres can be attributed to the relative paucity of nucleophilic sites in the fibre under the application conditions employed (Table 9.2), this being in contrast to the situation observed for reactive dyes on wool, for which deep shades can be secured as a result of a sufficient number of amine groups present in the two types of fibre (Table 9.7). Although the dyes are applied to PA fibres under weakly acidic conditions so as to maximise dye–fibre substantivity, since the pK_a of the amine conjugate acid $-(CH_2)_6-NH_3^+$ is ~10 [325], then the number of nucleophilic, unprotonated amino end groups (i.e. $-NH_2$) available for reaction with the dye will be low. Thus, although weakly acidic application conditions favour dye–fibre substantivity, they do not favour dye–fibre fixation. This is illustrated by the results obtained in a study [267] of the effects of pH on the exhaustion and fixation of a series of commercial modified vinyl sulphone reactive dyes on microfibre PA 66 (Figure 9.40).

Figure 9.40 shows that the extent of dye fixation, *%F*, of the dyes increased with increasing application pH over the pH range 3–8 because of a corresponding increase in the number of unprotonated, nucleophilic $-NH_2$ groups with which the dyes could react. Although the extent of total dye fixation, *%T*, followed the same pattern as that of *%F* in the pH range 3–6, at both pH 7 and 8, *%T* decreased owing to reduced dye exhaustion in the same pH region [267]. The conflicting requirements of dye exhaustion under acidic conditions and dye–fibre reaction under higher pH values were examined in the case of MCT/VS (monochlorotriazine/vinyl sulfone) heterobifunctional reactive dyes on PA 66 [326]. Pre-conversion of the unreactive VS precursor to the unsaturated, reactive VS moiety before dyeing resulted in higher fixation efficiency; conversion of the VS precursor as dyeing proceeds, by means of alkali addition subsequent to initial dye exhaustion, also enhanced fixation efficiency. The effects of optimising the application

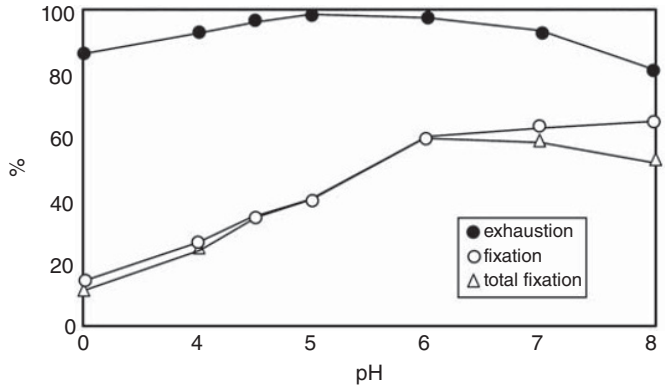

Figure 9.40 Exhaustion, % fixation and % total fixation achieved for 2% omf dyeings of *Stanalan Dark Red MFFN*. Reproduced from [267], with permission from Elsevier.

conditions used to apply four heterobifunctional reactive dyes to PA fabric have been determined in terms of the build-up of the dyes and the wet fastness of the ensuing dyeings [327].

In the late 1990s, interest attended the use of reactive dyes on PA fibres, mainly as a result of requirements for higher fastness dyeings on microfibre PA fibres. In order to achieve high wet fastness in full depths of shade, a modified PA 66 fibre of increased AEG content was introduced that enabled the provision of high wet fastness on PA fibres and commercial ranges of anionic reactive dyes intended for use on PA fibres were introduced [267]. A number of investigations have concerned the application of various types of reactive dye to PA fibres including chlorodifluoropyrimidinyl [328], α-bromoacrylamido [329], chlorotriazinyl and VS [330, 331], heterobifunctional [326, 327, 332], modified VS [267, 333], aminofluorotriazine [334] and monochlorotriazinyl [335, 336] types. For example, a study [337] employing seven commercial reactive dyes, which were intended for application to cellulosic fibres and which comprised the same chromophore and possessed one or more reactive group as well as between 1 and 3 chromophore units, revealed that dye fixation was not influenced by the degree of sulfonation of the dye and also that fixation was independent of both the number of chromophoric units and reactive centres present in the dye molecule, whereas the type of reactive centre was significant. The most important contributions to dye fixation appeared to stem from both the shape of the dye and the type of reactive group. The extent of fixation, on PA 66, of four mono-functional monochlorotriazinyl dyes that comprised the same chromophore but differed in their degree of sulfonation increased with increasing level of sulfonation [335]. For all the dyes used, fixation efficiency reduced markedly with increasing concentration of dye applied.

9.7.2 Disperse Reactive Dyes

In the late 1950s, ICI introduced a small range of reactive disperse dyes for PA fibres under the trade name *Procinyl*; the dyes were withdrawn in the 1980s [9]. Although the structures of the dyes were not disclosed, different reactive systems were employed. A blue AQ dye contained two 3-chloro-2-hydroxypropyl groups, a yellow azo derivative contained an aminochlorotriazine reactive group whilst the remaining dyes bore a 2-chloroethylsulfamoyl reactive group [338]. The dyes were applied using a two-stage process [339], namely initial exhaustion at pH 4 under which the dyes behaved as conventional (i.e. non-reactive) disperse dyes in their adsorption and diffusional behaviour, after which, covalent reaction with the fibre was achieved by increasing dyebath pH to 10.5. Evidence to support the notion that dye–fibre reaction had occurred was secured by the finding that the dyes could not be completely removed from dyed fibre by stripping using solvents [339]. The observation that dye uptake occurred in excess of the AEG content of the substrate (42.6 meq. kg^{-1}) was interpreted [339] as showing that the dyes reacted with not only AEG's but also amide groups within the PA substrate. However, as Peters suggested during the discussion of Scott and Vickerstaff's findings [339], a more likely explanation could be that the dyes may be able to react twice with each AEG.

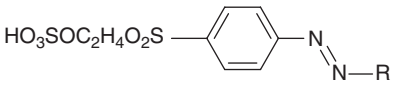

XVIII

The facts that the *Procinyl* dyes combined the properties of both disperse dyes (excellent coverage of fibre irregularities) and reactive dyes (high wet fastness) have been investigated by subsequent workers. For example, Dohmyou *et al.* [340] observed that maximum fixation of a dye of type **XVIII** on PA 6 fabric occurred at pH 8, this also being observed by Lo [341] in the case of dyes of general structure **XVIII**. In a subsequent study [342], reactive disperse dyes of general structure **XVIII** were found to display high wet fastness and excellent coverage of fibre irregularities when applied to both conventional and microfibre PA 66 fibre. This work [342] also demonstrated the feasibility of using disperse dyes on PA fibres that did not require formulation in the presence of dispersing agents. The use of such temporarily solubilised disperse dyes has been discussed in Chapter 8.

9.8 Sulphur Dyes

Although the use of selected sulphur dyes on PA blend materials, notably PA/cellulosic fibre blends, is well established (e.g. [343–345]), the application of the dyes to solely PA fibres has received little attention. Nevertheless, it has been shown that dyeings on PA fabric obtained using five sulphur dyes and two different reduction systems were of comparable colour strength to dyeings produced using the dyes on cotton [346]. The dyeings on PA 66 displayed very good fastness to repeated washing, which was enhanced by an aftertreatment with a commercial cationic fixing agent.

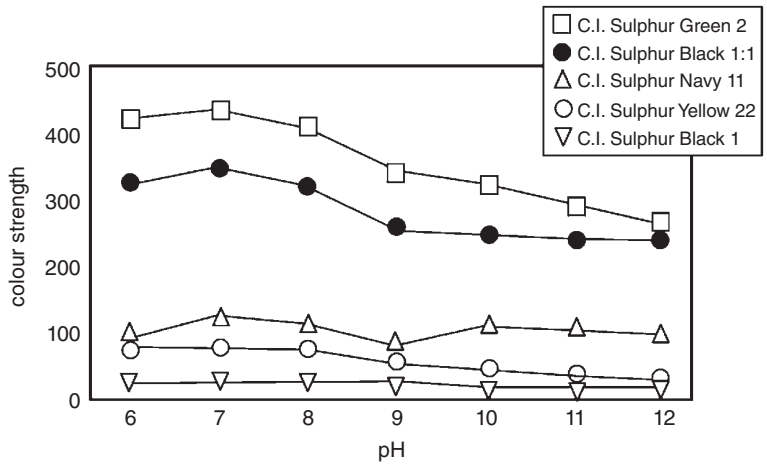

Figure 9.41 Colour strength as a function of application pH for dyeing at 98°C. Reproduced from [347], with permission from Elsevier.

Although the fastness of the dyeing to both the wet and dry rubbing was good, the dyeings displayed poor fastness to light. It was found [347] that, in the case of five sulphur dyes on PA 66 fabric, maximum colour strength was achieved at pH 7 and decreased with further increase in pH (Figure 9.41).

The effects of seven different reducing systems and three oxidation systems on the dyeing of PA 66 fabric using five commercial suphur dyes revealed [348] that the different reductants influenced both the colour and depth of shade of the dyeings. Although there was little difference between the three oxidising systems in terms of colour strength of the dyeings, the colour of the dyeings differed for the three oxidation systems studied. In an attempt to elucidate the nature of the sulphur dye–PA 66 fibre interaction, both C.I. Sulphur dyes and C.I. Solubilised Sulphur dyes were applied to four different types of PA 66 fabric, namely deep-dyeable, standard-dyeable, cationic-dyeable and acetylated variants [349]. The colour strength of the dyeings achieved on the four different types of PA 66 substrate was little influenced either by AEG content or the nature of the polymer from which the substrates had been derived. In addition, as the colour of the dyeings on each of the four types of fibre was similar, it was concluded that the interactions between the substrates and both sulphur dyes and solubilised sulphur dyes predominantly involved non-specific sites and therefore that dye–fibre substantivity can mostly be attributed to H-bonding, dispersion forces and polar van der Waals' forces of interaction.

9.9 Vat Dyes

The use of vat dyes on PA fibres is mostly confined to blends of the fibre with cotton and other cellulosic fibres [9]. In the case of 100% PA fibres, in 1939, Stott [191] reported the low substantivity displayed by the leuco form of vat dyes on PA fibres, which was attributed to the low diffusional behaviour of the dye anions within the substrate. More recently, it was observed that three vat dyes displayed very high levels of wet fastness on PA 66 supermicrofibre when applied as both the acid leuco and alkali leuco variants [300]. Although some vat dyes display low light fastness on PA fibres [191, 211, 350], which has been ascribed to low penetration and lack of aggregation of the dyes within the fibre [9], other vat dyes exhibit good levels of fastness to light on the substrate [7, 215].

9.10 Azoic Colorants

Azoic colorants can be applied to PA fibres using the conventional application method employed for applying the colorants to cellulosic fibres, although the shades obtained tend to be duller than those on cellulosic fibres (e.g. [9] and the references therein).

9.11 Microfibres

The topic of microfibres is discussed in Chapter 1. As the polymer used in PA microfibre is often the same as that employed in conventional decitex PA fibre, microfibres can be dyed in a similar manner to fibres of conventional linear density. This is demonstrated by the findings of Viallier and Jordan [239] who observed that the adsorption of C.I. Acid

Blue 113 and C.I. Acid Yellow 262 followed a Langmuir mechanism in the cases of both conventional and microfibre PA 66 fibres (Figure 9.25).

However, because microfibre has a larger surface area per unit mass of substrate than its conventional decitex counterpart, the greater extent of light reflected from the surface of dyed microfibre results in greater amounts of dye being required to achieve the same colour strength as that provided on conventional decitex fibres. This has been demonstrated by many workers in the cases of acid dyes, anionic reactive dyes and reactive disperse dyes (e.g. [239, 286, 316, 328–330, 342, 351]; see [9] and the references therein), as illustrated by the results shown in Figures 9.42, 9.43, and 9.44.

In a study using reactive disperse dyes [342], it was found that 25–33% more dye was required to achieve the same colour strength on microfibre than conventional decitex PA 66 fabrics.

Because more dye must be used to achieve the same visual depth of shade on microfibre as on its conventional decitex counterpart than for dyeings of the same colour strength, the wet fastness of dyed microfibre is generally lower than that of dyed conventional decitex fibre of similar depth of shade [316, 351]. Although aftertreatment with a syntan and syntan/cation system can be used to improve the wet fastness of dyed microfibre, such aftertreatments are generally less effective in the case of dyeings on microfibre [9, 286, 316]. Whilst the low wash fastness displayed by three 1 : 2 pre-metallised acid dyes on PA 66 super microfibre (0.06 dtex) was improved by an aftertreatment with the full back-tan, the level of fastness achieved still left much to be desired [300]. In contrast, the wash fastness of three vat dyes on the substrate, applied as both the acid leuco and alkali leuco variants, was much higher, despite the greater colour strength of the vat dyeings.

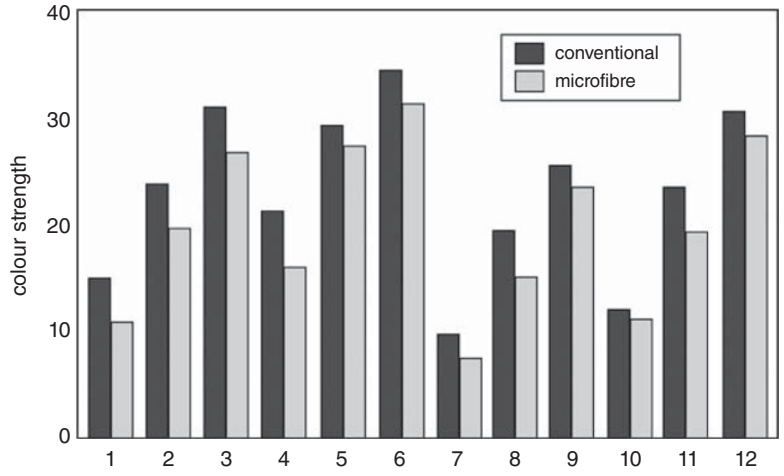

Figure 9.42 K/S of dyeings on conventional (78f46: 1.7 dtex) and microfibre (85f92; 0.9 dtex) PA 66 fabrics at 98°C. **1**: 1% omf, **2**: 2% omf, **3**: 4% omf C.I. Acid Blue 25; **4**: 1% omf, **5**: 2% omf, **6**: 4% omf C.I. Acid Blue 113; **7**: 1% omf, **8**: 2% omf, **9**: 4% omf C.I. Acid Red 119; **10**: 1% omf, **11**: 2% omf, **12**: 4% omf C.I. Acid Orange 127. Reproduced from [351], with permission from Elsevier.

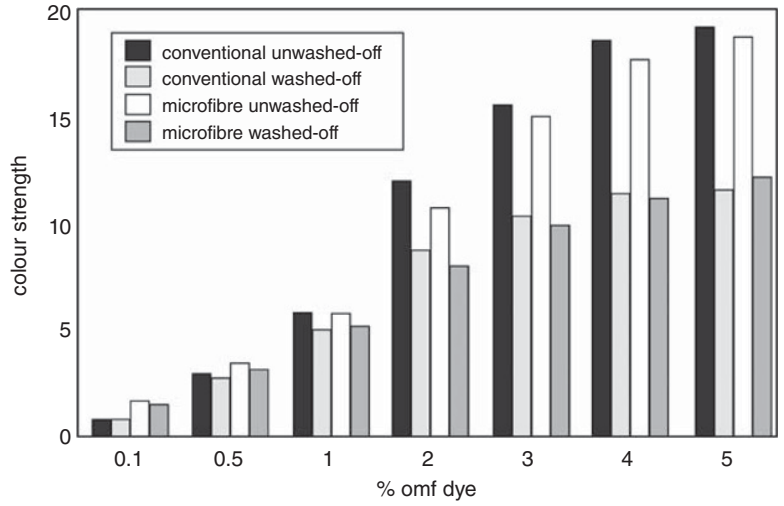

Figure 9.43 Build-up of C.I. Reactive Blue 114 on conventional (78f46: 1.7 dtex) and microfibre (60f68; 0.9 dtex) PA 66 fabrics at 95°C and pH 4 before and after wash-off. Reproduced from [328], with permission from Elsevier.

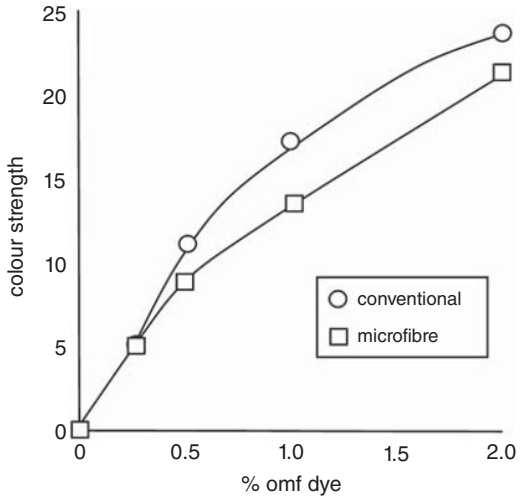

Figure 9.44 Build-up of a reactive disperse dye on conventional (78f46: 1.7 dtex) and microfibre (85f92; 0.9 dtex) PA 66 fabrics of identical AEG content (66.4 m eq. kg^{-1}) at 95°C and pH 8. Reproduced from [342], with permission from Elsevier.

Table 9.8 Melting and glass transition temperatures of some polyamides [357].

polymer	T_m/°C	T_g/°C
PA 6T/66	310	90
PA 6T/6I/66	312	125
PA 6T/DT[a]	300	140
PA 66	263	65

[a] *D* = 2-methylpentamethylenediamine; trade name *Dytek A* [22].

9.12 Semi-Aromatic Polyamides

Essentially, semi-aromatic polyamides occupy an intermediate position midway between aliphatic polyamides (e.g. PA 6 and PA 66) and aromatic polyamides (e.g. Kevlar and Nomex). Semi-aromatic polyamides are obtained by the combination of an aromatic monomer(s) (e.g. terephthalic acid, ***T***, and isophthalic acid, ***I***) with an aliphatic monomer(s) (e.g. hexamethylene diamine). The most commonly used aromatic monomer is terephthalic acid which, in combination with linear diamines, provides PA polymers that display generally higher T_m, higher T_g, lower moisture sorption and higher chemical resistance than their wholly aliphatic PA counterparts. As such, the performance of semi-aromatic polyamides lies between that of conventional engineering resins and high-performance polymers such as Kevlar and Nomex. Semi-aromatic PA's enjoy manifold applications (e.g. [353]), mostly as engineering components that are required to withstand very hot, very cold and chemically aggressive environments [354]; they are effective as a competitor to metals [354, 355].

Semi-aromatic polyamides are often considered as *poly(phthalamide)s*, *PPA's*, which are defined as *a polyamide in which the residues of terephthalic acid or isophthalic acid or a combination of the two comprise at least 55 molar percent of the dicarboxylic acid portion of the repeating structural units in the polymer chain* [356]. For accounts of PPAs, see e.g. [22, 353, 355, 357–359].

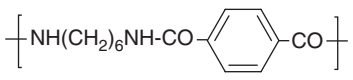

XIX

Both amorphous or semi-crystalline PPA's are available depending on the monomers employed, semi-crystalline variants being mostly based on PA 6T, **XIX**, which is obtained from hexamethylene diamine and terephthalic acid (T_m

(°C): PA 6T 370; PA 66 265 [359]). Many PPA's are copolyamides based on PA 6T, common examples being shown in Table 9.8.

9.13 Aromatic Polyamides

An aromatic polyamide or *aramid, AR*, fibre is *composed of linear macromolecules made up of aromatic groups joined by amide or imide linkages, at least 85% of the amide or imide linkages being joined directly to two aromatic rings and the number of imide linkages, if the latter are present, not exceeding the number of amide linkages* [360].

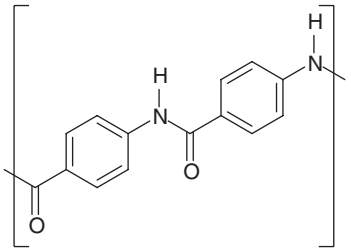

PMPI

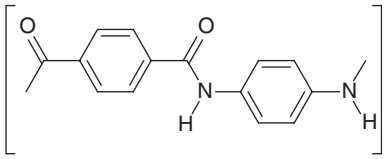

PPTAI

The first aramid fibres appeared in the 1960s with the introduction of the *m*-aramid fibre, poly(*m*-phenylene isophthalamide) (PMPI; aka MPIA; aka MPDI,[18] aka *Nomex*), which displays high-temperature stability and high resistance to degradation, with mechanical properties similar to those of PES fibre. In the 1970s, the aromatic, rigid rod, lyotropic liquid crystalline, *p*-aramid fibre poly(*p*-phenylene terephthalamide) (PPTA; aka PPDT; aka *Kevlar*) was introduced, which is characterised by outstanding mechanical performance coupled with high-temperature stability and resistance to combustion. Whilst several modified aramids and copolymers are available (e.g. [16, 17, 361]), this section focuses on the two homopolymers PMPI and PPTA.

The aramids enjoy several specialist applications[19] and are produced in various physical forms (fibres, non-wovens, films, etc.) (e.g. [16, 362, 363]) of which fibres are the most common [364]. Aramid fibres, in particular the *p*-variant, have received much attention (see the recent review [5]); details of the polymerisation and spinning of the fibres are available (e.g. [5, 16, 17, 362, 364–366]).

Both PMPI and PPTA materials are **AABB**-type polyamides that comprise amide groups (—NHCO—) separated by naphthalene and/or phenylene rings (represented by Ar′ and Ar″ in **XX**). The different properties displayed by PMPI and PPTA aramids arise from the different orientational positions (i.e. *meta* and *para*) of the amine and carbonyl moieties on the aromatic rings, which influence the crystal structure and intermolecular H-bonding ability of the two types of polymer.

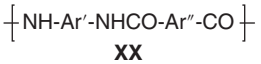

XX

Owing to the particular orientation of the —NH and —CO moieties in the *p*-aramid polymer, under appropriate polymerisation conditions (e.g. [16, 18, 365, 366]), the polymer solution assumes a liquid crystalline (aka anisotropic) nature rather than an isotropic character, resulting in the polymer chains adopting a rigid, rod-like crystalline configuration. During subsequent extrusion and processing, the polymer chains become highly oriented, which results in both significant anisotropy of physical properties (e.g. elastic modulus and thermal expansion coefficient) and high crystallinity (e.g. Kevlar 49 has a degree of crystallinity of 95% [364]). The *m*-aramid variant does not readily crystallise and, therefore, a fully oriented liquid crystalline structure is not formed and the ensuing fibres possess a partially crystalline, partially oriented structure similar to that of other solution-spun fibres [367].

In the context of their outstanding thermal properties, whilst aliphatic polyamides melt at <300°C (e.g. PA 6 ~230°C; PA 66 ~260°C) aramids either do not melt or melt >350°C [362], the decomposition temperature, T_d, of PMPI exceeding 450°C and that of PPTA >550°C [364]. However, debate attends whether or not aramids possess a T_m insofar as whilst decomposition temperatures have been observed, a value of 530°C has been recorded for the

[18] also referred to as poly(*m*-phenylene diisocyanate), MPDI.

[19] for example, *p*-aramid fibres are widely used for bulletproof vests and armour whereas the greater wearer comfort of the meta variants is reflected in their use in firefighter clothing.

T_m of PPTA [16, 364]. Values of ~272 and 95°C have been reported for the T_g of PMPI and PPTA [368],[20] which contrast markedly to the values of ~65–70°C in the cases of PA 6 and PA 66 (Table 9.4).

9.13.1 Fine Structure

9.13.1.1 p-*Aramids*

The crystalline nature of PPTA has received considerable interest (e.g. [16–18, 364, 365, 369, 370]). The crystal unit cell of the *p*-aramid is pseudo-orthorhombic [16], the molecular chains being fully extended in the crystalline regions [16]. H-bonds occur between adjacent polyamide chains (two H-bonds per unit cell length) and the ensuing H-bonded sheets are held together by van der Waals interactions (Figure 9.45). The close proximity of amide groups in adjacent chains provides relatively strong intermolecular H-bonding whilst the absence of significant free bond rotation around the —NH and —CO bonds results in the polymer chains assuming a rigid, rod-like character [16].

PPTA fibres display a high degree of crystallinity, with estimates of the degree of crystallinity of *p*-aramid fibres ranging from 68% to 95% [364]. However, the presence of amorphous domains is a matter of debate. For instance, whilst some authors consider that aramid fibres contain little or no amorphous regions [365, 372], it is considered that the absence of X-ray diffraction patterns characteristic of amorphous regions in Kevlar fibre does not mean that the fibre is 100% crystalline but, rather, that fibre crystallinity is very high and could not be determined exactly [373]. In contrast, a detailed analysis [374] of the crystallite structure and morphology of both fibre and as-polymerised polymer forms of three types of PPTA revealed that a heterogeneous, imperfect microcrystalline structure formed during processing, which was the origin of accessibility of small molecules.

The crystal structure of PPTA obtained from high polymer concentration is monoclinic with pseudo-orthorhombic symmetry [365]. PPTA fibres assume a complex, radial orientation of pleated H-bonded sheets (Figure 9.46) that plays a major role in determining the fibre's mechanical properties. PPTA fibres possess skin-core heterogeneity [90, 375], skin thickness being a characteristic of the particular fibre variant, ranging from a negligible presence in the case of Kevlar 149 to constituting ~60–70% of the total cross-section of Kevlar 981 [376]. The crystallites are less aligned in the core than in the skin [377]. X-ray diffraction studies revealed the presence of needle-shaped microvoids in Kevlar PPTA fibres [91], ~12 nm long and ~2.5 nm wide, that were aligned parallel to the fibre axis and distributed in the skin around the periphery of the fibres; Kevlar 49 fibres contained 3.4% voids [378]. A correlation was observed between microvoid or skin content and fibre strength [379].

A schematic representation of the microstructure of PPTA fibre is shown in Figure 9.47. The *p*-aramid fibre is composed of a parallel array of fibrils ~60 nm diameter, each consisting of a series of crystallites arranged end to end; polymer molecules can populate more than one crystallite [365]. Microfibrils in PPTA fibres have been estimated as being 7–10 nm in diameter [90].

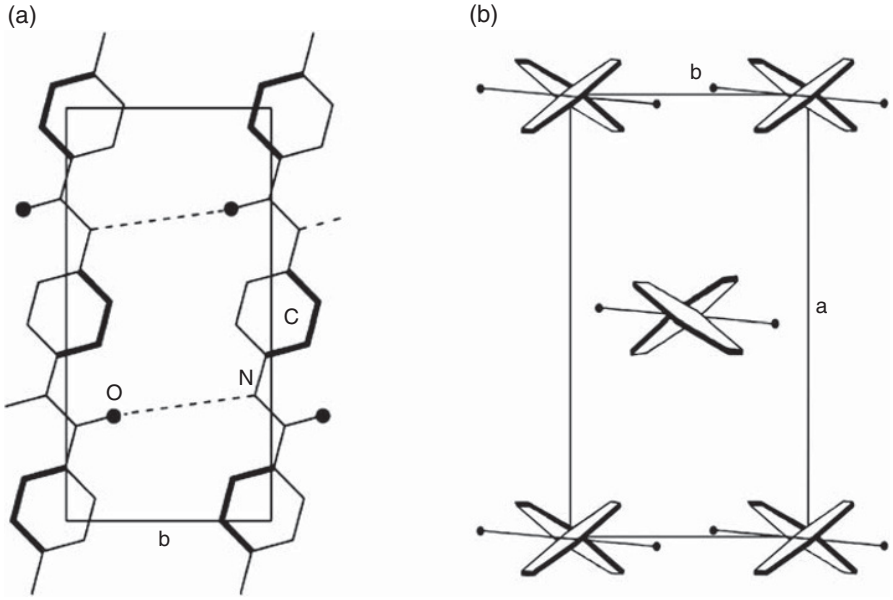

Figure 9.45 Crystal structure of PPTA: (a) side view along the *a*-axis and (b) top view along the *c*-axis. Reproduced from [371], with permission from John Wiley & Sons, Inc.

[20] though T_g determination is difficult in the case of PPTA owing to its essentially 100% crystalline nature [364].

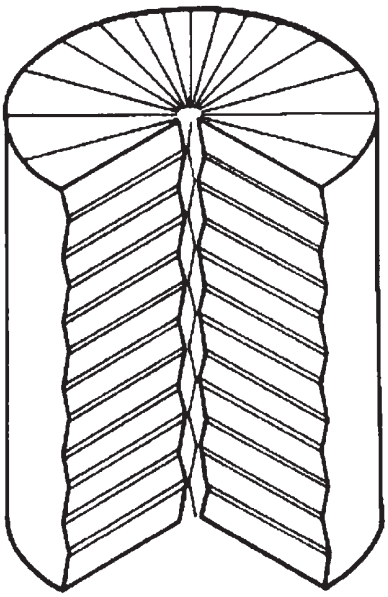

Figure 9.46 Schematic representation of Kevlar 49 fibre showing the radially arranged pleated sheets. Reproduced from [375], with permission from John Wiley & Sons, Inc.

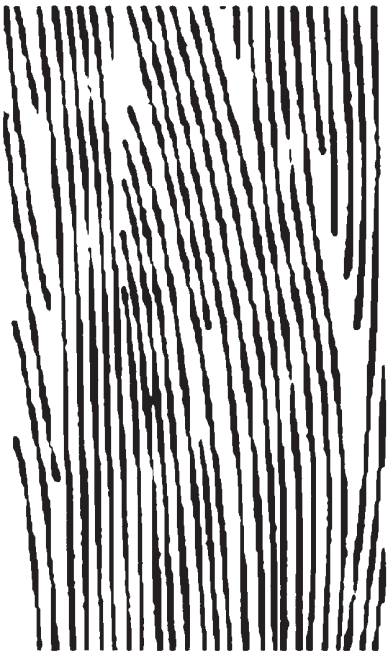

Figure 9.47 Schematic representation of PPTA fibre. Reproduced from [366], with permission from Elsevier.

9.13.1.2 m-*Aramids*

Much less attention has been focused on this isomer, which has a triclinic unit cell, in which the chains are prevented from assuming a fully extended conformation [16]. H-bonds occur between adjacent polyamide chains (one H-bond per unit cell length) and the ensuing H-bonded sheets are held together by van der Waals interactions (Figure 9.48). The PMPI polymer is less linear than PPTA and therefore displays lower crystallinity [5, 364].

9.13.2 Water/Aramid Interactions

Both *m*- and *p*-aramid fibres are hygroscopic, reported values of moisture regain being 5.2% in the case of PMPI and 3.7% for Kevlar 49 at 65% RH [362]; indeed, the hygroscopicity of Kevlar 29 and 49 (4% and 7% at 65% and 100%

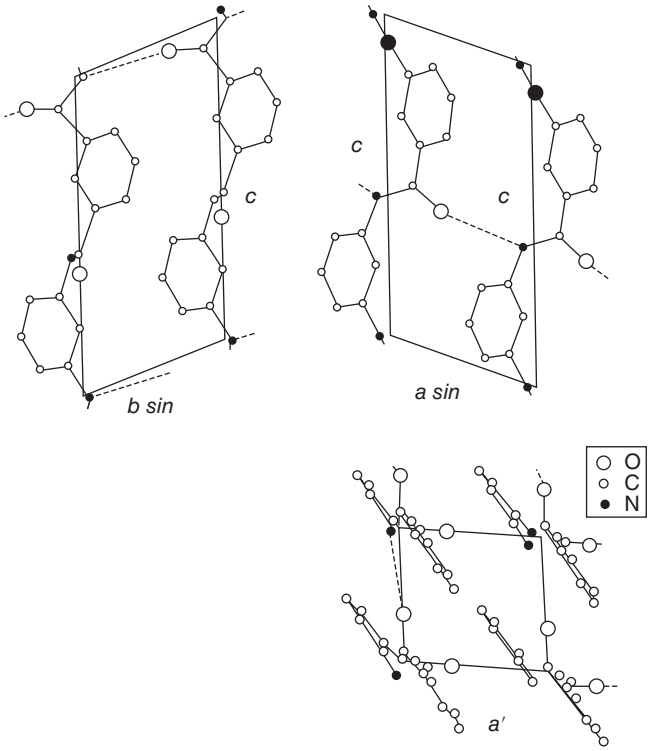

Figure 9.48 Crystal lattice of PMPI. Reproduced from [16], with permission from Elsevier.

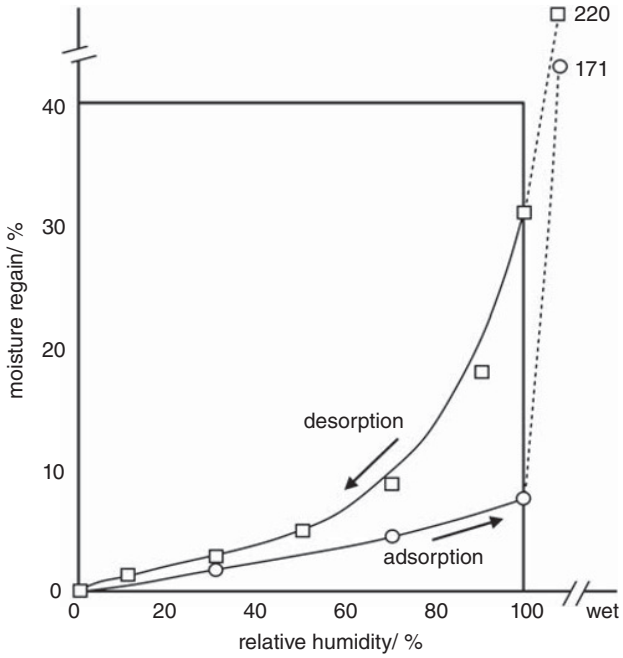

Figure 9.49 Moisture adsorption and desorption isotherms for as-spun PPTA fibre. Reproduced from [393], with permission from John Wiley & Sons, Inc.

RH, respectively, at 30°C) is similar to that of PA 6 and PA 66 [380]. Moisture sorption isotherms for aramid fibres are sigmoidal in shape [380–382] and moisture sorption displays hysteresis [382] (Figure 9.49).

Interpretation of such moisture sorption using the BET multilayer adsorption model that assumes different numbers, n, of layers of sorbed water molecules revealed three kinds of moisture regain at a given RH, namely Langmuir monolayer adsorption ($n = 1$), BET multilayer adsorption ($n_{max} \geq n > 1$) as well as a further type of sorption mechanism ($n > n_{max}$), such as water clustering or condensation [380]. The moisture regain value of n_{max} was found to be 6–7 and the

amounts of the three kinds of sorbed water were 1.5%, 4.2% and 1.7% for $n = 1$, $n_{max} \geq n > 1$ and $n > n_{max}$, respectively, at saturated vapour pressure [380].

p-Aramid fibres typically shrink little in boiling water [383], do not swell in water [377] and have no measurable porosity [382], the latter characteristic going some way to explaining the fact that water diffusion rates ($\sim 5 \times 10^{-12}$ $cm^2\ s^{-1}$ at 28°C) in Kevlar 49 were found to be much lower than in other polymers [382].

As mentioned, aramid fibres are highly crystalline. In the case of other semi-crystalline fibres and polymers (e.g. PA 6 and PA 66), water sorption is confined to the amorphous regions of the polymer and involves the amide groups. However, as discussed earlier, in the case of aramid fibres, the presence of amorphous domains has not been entirely resolved. Furthermore, whilst the moisture sorption character of *p*-aramid fibres accords with the fact that the fibres have similar amide group content as PA 6 and PA 66 fibres, the water sorption behaviour of PPTA fibres does not concur with the fact that the crystallinity of the aramid fibres is far greater than that of PA 6 and PA 66 [380]. As X-ray data have shown that sorbed water does not penetrate the unit cell of the crystal lattice of PPTA fibres [372], three possible explanations have been proposed to describe the mechanism by which water sorption occurs in aramid fibres, namely water/amide group interactions, water-filled microvoids and adsorption of water by hydrophilic inorganic salts in the substrate.

The question as to whether water/amide group interactions occur in aramids has not been entirely resolved insofar as IR and NMR evidence provide contradictory results [384]. Furthermore, WAXD studies suggest, qualitatively, that sorbed water may interact with ─CONH─ groups in the outermost chains of crystallites [381]. Fukuda and Kawai [90] proposed that, in Kevlar fibres, water molecules are adsorbed onto amide groups at the chain ends, intrafibrillar lattice deficits and inner surfaces of microvoids. At low vapour pressures, small clusters of water molecules form that, at high vapour pressures, grow to fill the microvoids. ^{13}C NMR analysis suggested that water sorption in PPTA fibre imparted no major changes to the chemical structure of the fibre during hydration, whilst ^{1}H NMR spectra revealed that essentially all the absorbed water was loosely bound; evidence was obtained that was indicative of a slight increase in plasticity of the fibre after hydration [384]. Water was found to be located at two sites in PPTA fibre, the sites differing in terms of the level of constraint that they imparted to the motion of water molecules. Based on the existence of microvoids in PPTA fibres [376], the two sites were assigned to two different sizes of void in the substrate, the smaller voids more rigidly constraining the water molecules [384]. In the context of the multilayer adsorption mechanism discussed earlier, it has been proposed [92] that initially water molecules are tightly bound to adsorption sites with $n = 1$ (i.e. monolayer adsorption) and that further water molecules bind loosely to the adsorbed water molecules forming a micro-water cluster (with $n_{max} \geq n > 1$) (i.e. multilayer adsorption). If sufficient microvoid space is available, the micro-water clusters grow to form macro-water clusters until the microvoids are filled with condensed moisture [92].

Aramid fibres typically contain small amounts of inorganic salts (e.g. Na_2SO_4 [378, 385, 386] or Na_2CO_3 [384]) that are formed in the fibre during fibre processing (e.g. [377, 378]). For example, Kevlar 49 fibres were found to contain 15 000–17 000 ppm impurities, of which 50% was $NaSO_4$ located between the fibrillar, 60-nm diameter crystallites [378]. Clusters of Na_2SO_4 are considered a source of microvoid formation, Kevlar 29 fibres having been found to contain 0.8% of 10-nm diameter spherical microvoids that become ellipsoidal in shape ($10 \times 5 \times 5$ nm) as a result of orientation [378]. As Na_2SO_4 is a desiccant, it was suggested that its presence in the fibre could possibly contribute to water sorption [373] and also may contribute to fibre fracture associated with water sorption [386]. In the case of Kevlar 49, water accrues preferentially within interfibrillar regions in which clusters of Na_2SO_4 and their associated microvoids reside [378]. It was suggested that microvoids in the fibre contain mostly Na_2CO_3 and, depending on the fraction of the pore initially filled with the salt, sorbed water may either fully or partially dissolve the Na_2CO_3 [384].

9.13.3 Dyeing of Aromatic Polyamide Fibres

Owing to their high crystallinity, high orientation and high T_g, aramid fibres are very difficult to dye. Indeed, both the *m*- and *p*-variants are dyed almost exclusively using selected basic dyes as both types of fibre display little if any substantivity towards other classes of dye. The dyeability of *m*-aramid fibres has received more attention than that of the *p*-variant.

The application of basic dyes to Nomex-type fibres is typically undertaken at high temperatures (~120–130°C) in the presence of high amounts (~40% omf [387]) of selected carriers such as benzyl alcohol [388] for long dyeing times. Several approaches have been used in an attempt to increase the substantivity of the fibre towards the dyes, including, for example, pre-treatment with various compounds such as organic solvents [389, 390], liquid NH_3 [391], amines [392, 393], as well as photo-oxidation using UV/ozone [394, 395] and the use of organic solvent dyeing [387, 396]. More recently, the application of disperse dyes from sCO_2 has been examined [397, 398]. The dyeing of *p*-aramid fibres with basic dyes is typically carried in the absence of carrier at 180°C [387], various pre-treatments having been investigated to enhance dye uptake (e.g. [387, 399]).